Stockholm University

Bachelor Thesis

Degree Project in Geology 15 hp

Identification of the host rocks and the environment of formation of the Liikavaara Cu-Au deposit, Norrbotten, Sweden

Madelen Estholm

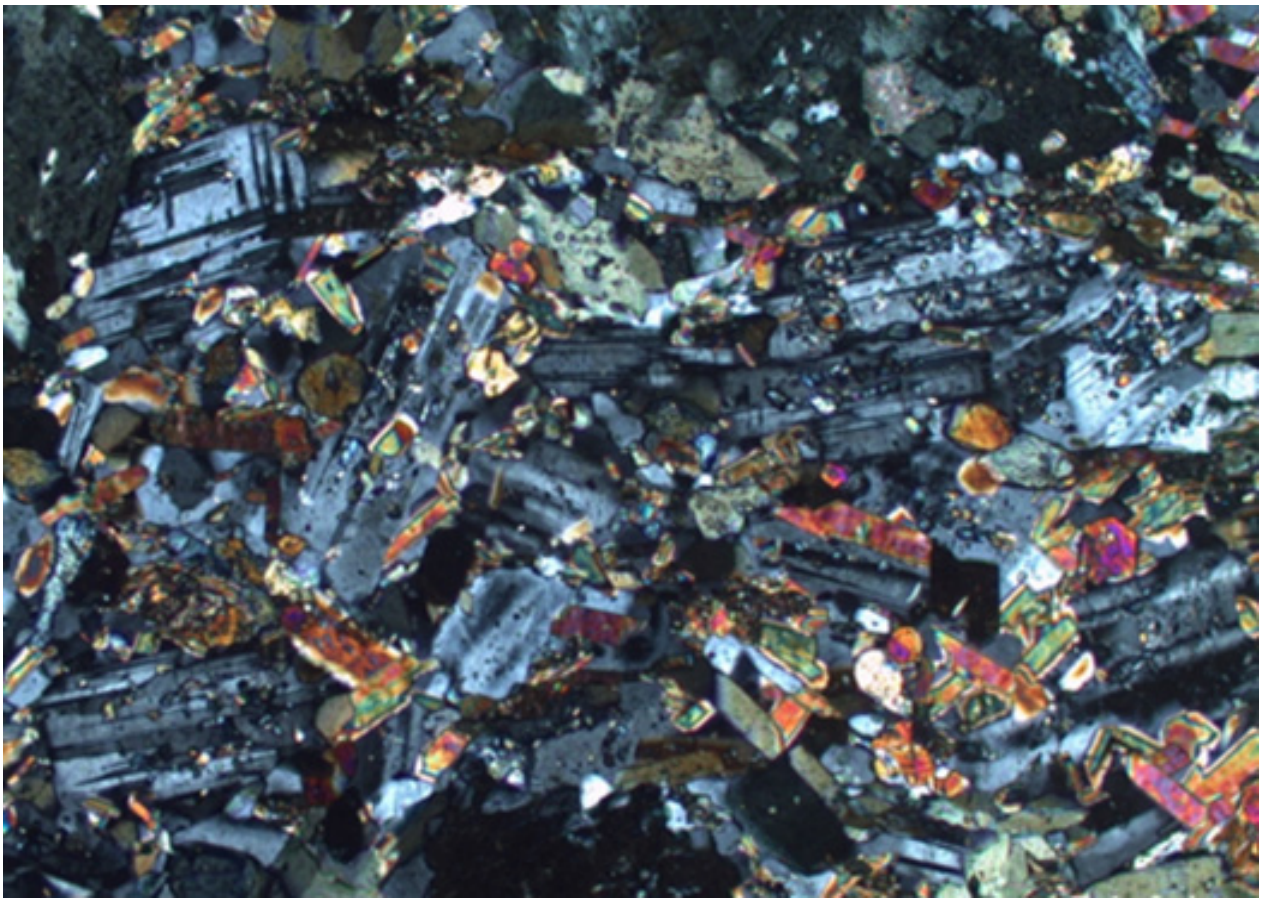

Stockholm 2014

Department of Geological Sciences
Stockholm University
SE-106 91 Stockholm

Identification of the host rocks environment of the Liikavaara Cu-Au deposit, Norrbotten, Sweden

Madelen Estholm

Bachelor thesis, 15 credits
Department of geological sciences, Stockholm University

Abstract

Northern Norrbotten is one of three important ore districts in Sweden. Norrbotten Archean craton has a history of convergent tectonic events and evolution of subduction processes. Since the evolution during the Precambrian eon, the area has not been experiencing or been affected by any larger collisions which has preserved the old geological history including mineral resources. The mineral recourses of iron, copper and gold are dominantly situated in the Gällivare and Kiruna areas. The mineralization processes in the area are not well understood. For classifying and understanding ore deposits a key is to identify the host rock and environment of formation. The subeconomic Liikavaara Cu-Au deposit, situated in Norrbotten, Sweden, is an unexcavated deposit. Previous research suggests a metamorphic rock of sedimentary origin with conglomerates and grading bed structures. Uncertainty arise in evaluation of the geochemical data which point instead a volcanic origin of these rocks. This study involves systematic examinations of two cores from the Liikavaara deposit, which were undertaken for identification of the immediate host rock environment. A description of macroscopic, microscopic and geochemical data was obtained for the cores. The geochemical results are used to preform normative calculation of the theoretical mineralogy of the aphanitic rock. The host rock is deformed, but preserves primary features such as euhedral plagioclase and relic igneous zoning. These are evidence that the host rock is of volcanic origin. This petrographic evidence is supported by the geochemical data which indicates that the host rock is of andesitic composition. Based on petrographic textural and geochemical data, I concluded that the host rock comprise pyroclastic debris and lava flows of andesitic composition. These rocks are typical of a suduction zone and this is proposed as a tectonic setting for ore formation. Subsequent deformation and metamorphism occurred at green schist facies conditions. A later intrusion also cuts the host rock, but this is also metamorphosed at green schist conditions. I thus conclude that the host rock of Liikavaara or deposits are of igneous not sedimentary origin in contrast to previous work.

Contents

1. Introduction 3

1.2 Previous research 4

1.3 Aim of project 4

1.4 Study area 5

1.5 Regional geology and tectonics 5

1.6 Sampling 7

2. Methods 9

2.1 Graphic logging 9

2.2 Preparation of thin section 9

2.3 Petrography 9

2.4 Geochemical whole rock analysis 9

2.5 Normative Calculation 10

2.6 Rock classification 10

2.6.1 IUGS classification 10

2.6.2 Classification of magma series 10

2.6.3 Pyroclastic classification 10

2.6.4 Metabasalt projection 10

3. Results 11

3.1 Graphic logging 11

3.2 Petrography 12

3.2.1 Macroscopic 12

3.2.1.1 Hanging wall 12

3.2.1.2 Mineralization zone 13

3.2.1.3 Footwall 14

3.2.2 Microscopic 15

3.2.2.1 Mineralogy 15

3.2.2.2 Textures 16

3.3 Geochemical analysis 20

3.4. Normative calculation 21

4. Discussion and interpretation of results 22

4.1 Interpretation of the host rock 22

4.2 Environment of formation 26

4.3 Metamorphic petrology 26

4.4 Evaluation of methods 27

5. Conclusion 28

6. Acknowledgements 28

7. References 29

8. Appendix 30

1. Introduction

Sweden is a country with a long history of mining and exploration. The Falun copper mine, for example, has been mined since the 9th century or even earlier (Eriksson and Quarfort, 1996). Today in Sweden, there are three main mining districts: Bergslagen, Skellefte field and Malmfälten. Malmfälten in northern Norrbotten is an important district that hosts a large apatite iron deposit in Kiruna and the porphyry copper-gold-silver deposit in Aitik, situated 15 km east of Gällivare (Figure 1). The Gällivare area has a history of mining since the discovery of the Malmberget iron deposit in the 18th century, followed by the discovery of the copper deposit in Nautanen (5 km northeast of Gällivare district) which is under exploration by Boliden AB today.

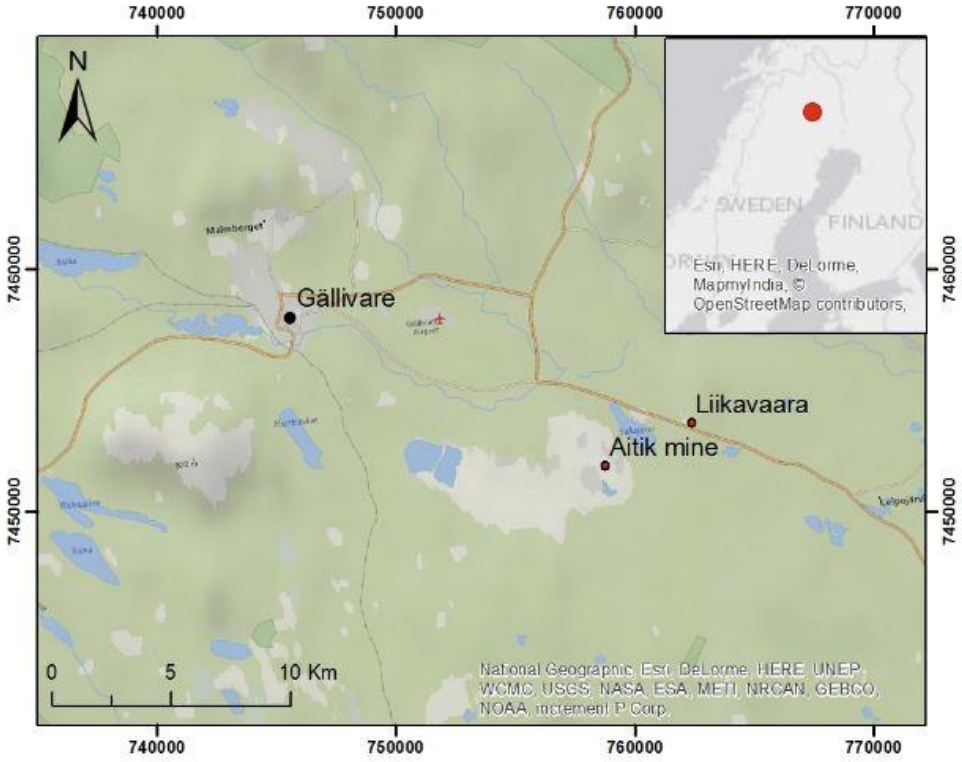

Figure 1. *Map of Gällivare area.*

Boliden AB has a history of exploration of mineral deposits since the 1920s in the Skellefte field (south of Norrbotten) (Boliden annual report 2013, 2014, p.41). Boliden discovered the Aitik and nearby Liikavaara copper and gold deposits in 1932 by tracking boulders containing disseminated chalcopyrite (Zweifel, 1976). The Aitik deposit came into production in 1968 (Zweifel, 1976). Aitik is a metamorphosed porphyry copper deposit with a later IOGC-mineralization overprint (Wanhainen et al., 2012). Today, although this deposit consists of a low grade copper ore (Boliden annual report:2013, 2014 p. 38), it is the largest open pit mine in Sweden due to its size and ore production of 37 Mton during year 2013 (Boliden annual report: 2013, 2014. p 38).

The copper-mineralization processes in the Gällivare area are specific to the Norrbotten region and are not well understood (Bergman et al., 2001). Several epigenic copper deposits have been found in the Gällivare area, but few of them are of economic value (Bergman et al., 2001). The subeconomic copper-gold deposit of Liikavaara (termed Liikavaara East by Zweifel, 1976) is situated 3 km east of Aitik and has not yet been mined. It is not comparable to the Aitik deposit, which is distinctively larger in size. Zweifel (1976) conducted investigations at both the Liikavaara and Aitik to classify the ore deposits. Since then several studies and interpretations have been proposed with the aim of classifying and understanding the Aitik area (Yngström et al., 1986; Wanhainen et al., 2012). However, in the Liikavaara area there are no recent scientific studies published since Zweifel´s primary investigation.

1.2. Previous research

An important aspect of classifying and understanding ore deposits is to identify the host rock and environment of formation. The primary investigation of the host rock of the Liikavaara Cu-Au deposit was suggested to be of a meta-sedimentary origin (Zweifel, 1976). The meta-sedimentary classification is an interpretation based on observed mineralogy, consisting mainly of feldspar and quartz, as well as sedimentary structures, such as conglomerates, cross beddings and graded beds**.** Zweifel (1976) identified amphibolitic layers in the rock, which were interpreted to be of sedimentary origin because they were thought to contain sedimentary clasts. The amphibolitic layers are suggested to have been created by a more dolomite rich sedimentation (Zweifel, 1976).

Zweifel (1976) also mentioned that the host rock would be better defined as a volcanic rock by interpretations of geochemical data, but suggested that the rock lacks mineralogical and textural evidence for a volcanic classification. Bergman et al. (2001) proposes that the copper deposits in Norrbotten and Gällivare region occur mostly in the Svecofennian rocks of volcanic origin.

1.3 Aim of project

The aim of this BSc thesis is to identify the host rock within Liikavaara Cu-Au deposit, Norrbotten, Sweden. More specifically, the objective is to decide if the host rock is of meta-sedimentary or meta-volcanic origin, and suggests a likely environment of formation. This was achieved by investigating two cores, which represented a stratigraphy of the host rock of Liikavaara Cu-Au deposit. A petrographical study of primary features by macroscopic and microscopic observations of the least altered lithology of the host rock is presented in this thesis. Also, an interpretation of geochemical data is made to characterize the origin of the host rock.

The result of this thesis can be useful for further studies by Boliden AB, to investigate alterations related to the mineralization and vein intrusions in the rock. Furthermore this thesis can contribute to a continued process of more accurate classification of the deposit, as well as better understanding of how and why the Liikavaara Cu-Au deposit was formed where it is situated today.

1.4 Study area

Liikavaara Cu-Au deposit is situated 16 km southeast of Gällivare, Sweden, and 3 km east of Aitik open pit mine (Figure 2). The deposit is named after the adjacent village, Liikavaara, situated at 7452961 N, 0762540 E (SWEREF 99 TM).

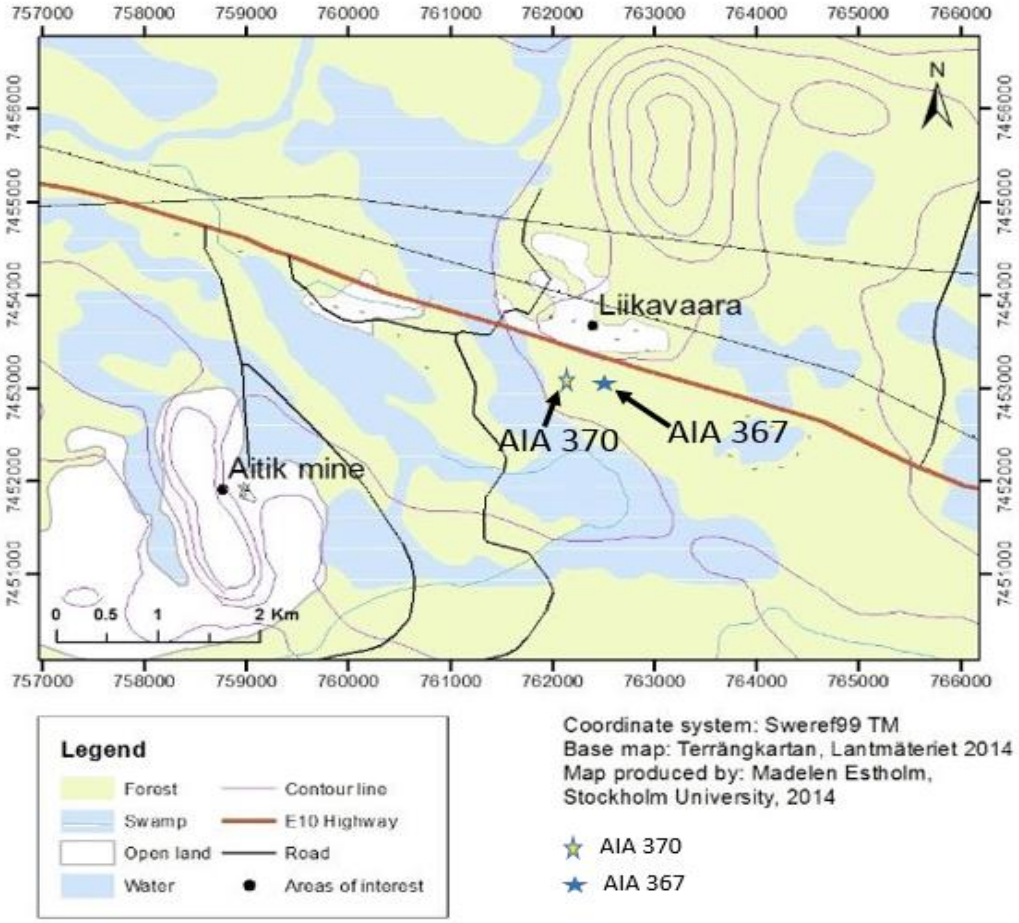

Figure 2. *Map of study area and geographical positions of examined cores AIA 367 (7452961 N, 0762540 E) and AIA 370 (7452966 N, 0762128 E). The village Liikavaara is marked on the map as Liikavaara.*

1.5 Regional geology and tectonics

The bedrock of northern Norrbotten was mainly formed during the middle Precambrian eon, 2.8-1.8 Ga (Bergman et al., 2001). The dominant orogenic processes: subduction and rifting, occurred during Archean and Palaeoproterozoic times (Weihed et al., 2005). The Norrbotten Archean craton along with the supracrustal metamorphic and magmatic rocks, have a history of repeated collision and extension (Weihed et al., 2005; Lehtinen et al., 2005). These tectonic events are linked to volcanic and pyroclastic rock deposits, which were metamorphosed during the Svecokarelian orogeny (Weihed et al., 2005).

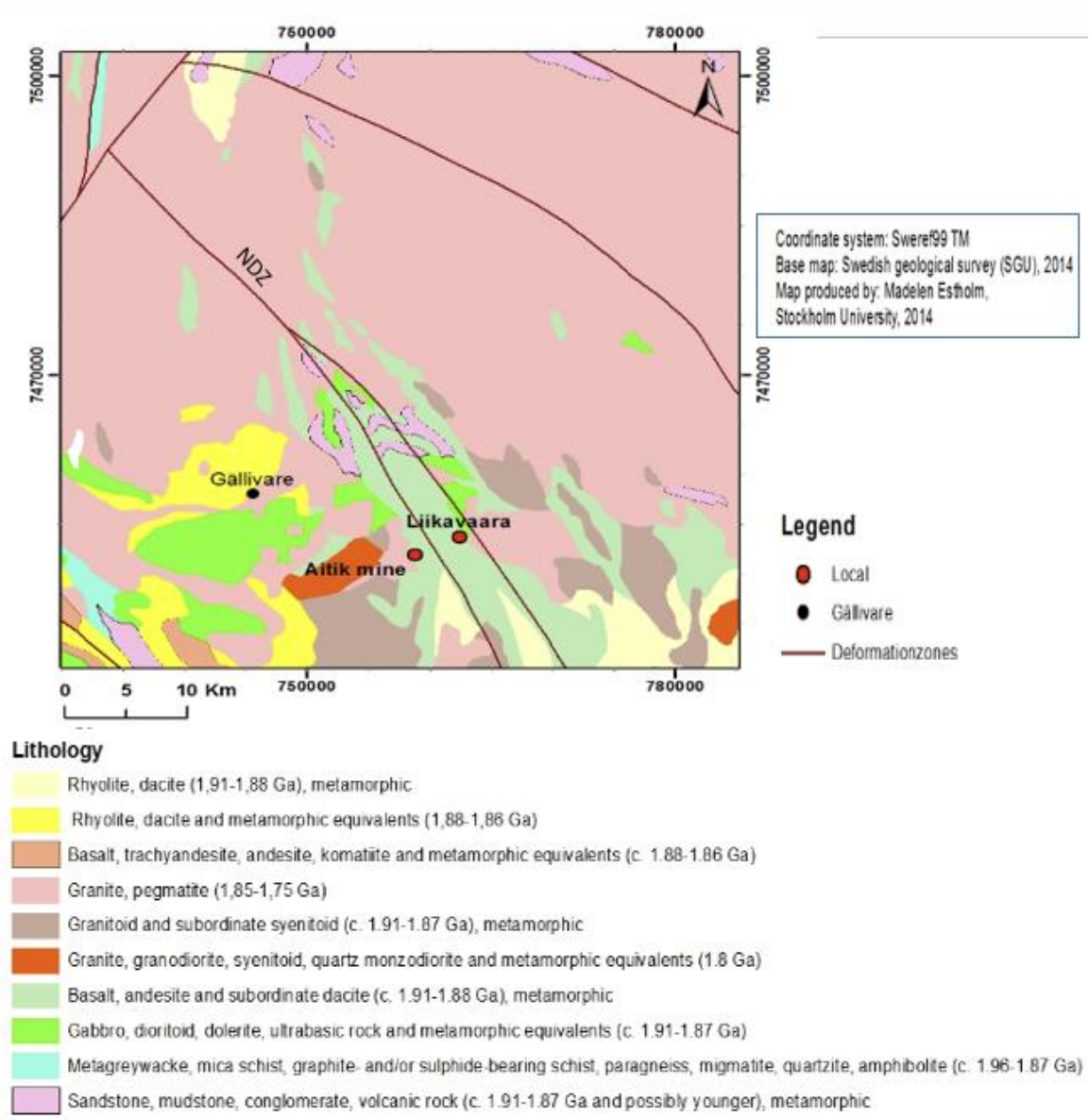

Figure 3. *Bed rock map of Northern Norrbotten (1.96-1.75 Ma).*

The Archean craton is classified as a granitoid gneiss and is partially exposed in the northernmost part of Norrbotten (Bergman et al., 2001). The craton is covered by a Karelian (2.3-196 GA) metabasalts and younger Svecofennian supracrustal rocks from Palaeprotozoic (Bergman et al., 2001). The Svecofennian supracrustal rocks (1.96-1.85Ga) are considered to be meta-volcanic rocks, commonly of intermediate, andesitic and calc-alkaline composition (Bergman et al., 2001). Rocks from the Svecokarelian orogeny formed at 1.9-1.8 Ga., included by sedimentary rocks, bimodal volcanism and intrusions (Figure 3) (Weihed et al., 2005; Bergman et al., 2001). Northern Norrbotten is crossed by three larger deformation zones: Karesuando-Arjeplog deformation zone, Pajala shear zone and Nautanen deformation zone (NDZ) (Bergman et al., 2001). The NDZ is crosses close to the Liikavaara deposit.

The Liikavaara and Aitik area is mainly flat with a few outcrops exposed, with the main soil cover consisting of till and “swamps” (Zweifel, 1976). Interpretation of Zweifel (1976) the deposit is suggested to be located on the eastern side of a synform with a SSE dipping axis. The rock of the Liikavaara group are of low metamorphic grade with increasing alteration and metamorphism towards the west and the Aitik area (Zweifel, 1976).

1.6 Sampling

The area is interpreted as a fault zone by Boliden AB (Höglund, 2014)(Figure 4). Boliden AB collected the cores AIA 370 and AIA 367 in year 2010 (Höglund, 2014). The graphic logging of sections was made on rocks that are not overprinted by extensive mineralization, veining or alteration. For the petrographical study, samples of different clasts and of the groundmass were collected. Samples for the geochemical analysis were collected from intervals of the most homogenous and least altered rocks from the host rock (Figure 5).

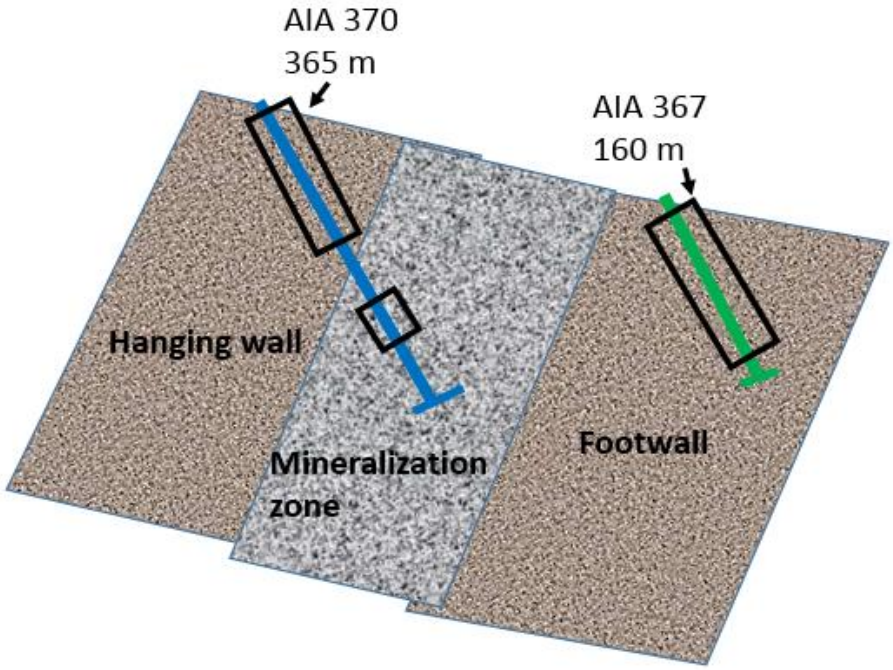

Figure 4. *A schematic sketch of the host rock in cross section featuring approximate length of the cores and sampling sections (black boxes). Modified from core sketches made by Sofia Höglund, geologist at Boliden AB (Höglund, 2014).*

Core AIA 370 is (Figure 2) 365 m long. The core was documented by graphic logging, sampling of 24 thin sections and collecting of 17 geochemical samples within the core interval of 5.7 to 160 m (Figure 5). This section represents the hanging wall within the fault zone. Further down the core at 269 to 285 meters, a less altered lithology was identified in the otherwise highly altered mineralized zone. Within this section, three thin sections and three geochemical samples were collected (Figure 5).

The second core (AIA 367) measures 160 m (Figure 2). This core represents the lithology of the footwall (Figure 4). The core was documented by graphic logging (5.6-160.4 m) and sampled of four thin sections and three geochemical samples (Figure 5).

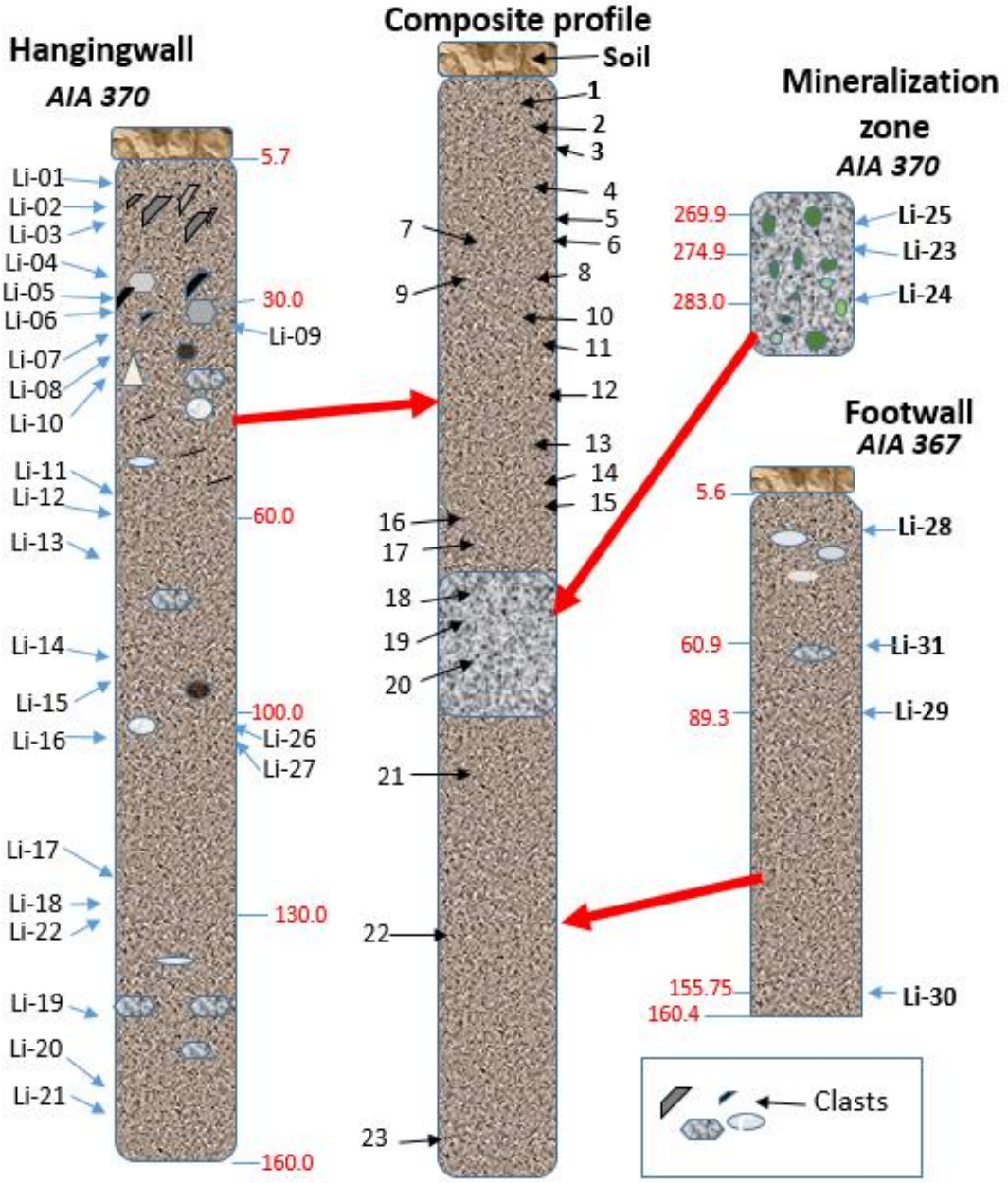

Figure 5. *Simulated composite profile of the three sampling sections from core AIA 367 and AIA 370. A soil cover of approximate 5.7 m cover the bed rock of selected cores. It illustrates where samples were collected for thin sections (Li-numbers Li-01 to Li-31) and geochemical analyses (numbers 1 to 23, in black). Red numbers show core depth of the different lithological units. Scale of core section, clast size and clast position are not accurately scaled .The accurate sampling depth can be obtained in table 7, Appendix.*

2. Methods

Different methods have been used to gain information from the selected drill cores provided by Boliden AB in Gällivare. This section gives a brief description of the methods in the order that they have been applied. These are: 1) Graphic logging of cores for a general overview of the stratigraphy, gathering data of clast contents and sampling for petrographic and geochemical analysis. 2) Macroscopic description of hand specimen to compare with the microscopic observation. 3) Petrographic study of polished thin section in microscope for description and identification of mineralogy and textural relationship to compare with geochemical data. 4) Geochemical characterization of whole rock analysis of major and minor elements to deduce the origin and suggest a potential environment of formation.

2.1 Graphic logging

Systematic documentation of estimated amounts of clast and their size was examined in one-meter sections in order to core depth. The observed clasts were defined as sand (0.5-2mm), pebbles (2mm-64mm) and cobbles (>64mm). The estimated amount of clast were accounted in percent.

2.2 Preparation of thin section

The selected samples were cut out to rock chips (20x35 mm) using a rock saw at Stockholm University. The rock chips were sent to Vancouver Petrographic's Ltd. in Canada to create 30 μm thick polished thin sections.

2.3 Petrography

Observation and description of hand specimen and thin sections provided detailed information about mineralogy and microtextures. This information was used to learn about the environment, of formation and metamorphism of the rock. The hand specimens and thin sections were systematically observed and described. The thin sections were observed in transmitted and reflected light in a petrographic microscope (Nikon, eclipse 50iPOL) at Stockholm's University.

2.4 Geochemical whole rock analysis

Geochemical whole rock analysis of major and minor elements is useful for characterizing and classifying igneous rocks when modal content is difficult to obtain in the rock. The collected samples (approximately 40 x 150 mm) were sent to ALS core service laboratory in Piteå, Sweden. In Piteå the 23 samples were crushed, pulverized (10 g pulp) and shipped together with standards, for ICP-ES (inductively coupled plasma emission spectrometry) analyses, to ACME laboratory in Canada.

The ICP-ES instrument is used to detect and to determine the major and minor elements in weight percent (wt %) that comprise the rock sample (Standard STD SO-18 in table 8, in appendix). The precision of the geochemical results is better than +/- 5%. This is due to variation of instruments and standards.

One clast observed in hand specimen was compared to the groundmass by XRF spectrometry. The clast was separated from the groundmass by using a rock saw. Both clast and groundmass were crushed for XRF spectrometry at Stockholm University (Standard, Stdcalib0313 at table 8, in appendix).

2.5 Normative calculations

Normative calculations were used to determine a theoretical mineralogy of the fine-grained rocks. The calculations were made in a spread sheet created by Hollocher K. (2014) (cited in Johannsen, 1931 p. 246). The major and minor elements were used from the geochemical data and LOI-normalized so as to enable the igneous protolith to be determined. The idealized mineralogy obtained from normative calculations is estimated to be of an igneous rock of anhydrous basis from a low pressure environment.

2.6 Rock classification

2.6.1 IUGS classification

The International Union of Geological Sciences (IUGS) classification by Le Bas and Streckeisen, (1991) where the geochemical data is used for characterization and classification of the origin igneous rocks by international standards. Total alkali (Na2O+K2O) versus silica (SiO_2) (TAS) diagram (Le Maitre, 1984) was applied after the IUGS classification scheme.

2.5.5 Pyroclastic classification

Pyroclastic classification method is used by Fisher (1966), to classify pyroclastic content (%) and by their size (mm). The classification is made of the one-meter sections from the graphical loggings.

2.6.2 Classification of magma series

Classification of magma series is based on the rocks chemical composition (Irvine and Baragar, 1971). Magma series is divided into alkaline versus subalkaline field, based on silica (SiO_2) wt% and alkali (Na2O+K2O) wt%. An AFM-ternary diagram (Irvine and Baragar, 1971) was used for further subdivision of magma series.

2.6.3 Metabasalt projection

An ACF-diagram was created from the geochemical data in a three component system (Philpotts and Ague, 2009). Calculations of geochemical data were based on: A=Al2O3+Fe2O3 – (Na2O + K2O), C=CaO+3.3*P2O5 and F=FeO + MgO + MnO. Fe2O3 was converted to FeO (Fe2O3*0,8998) (Winter, 2010). For these calculations the data were recalculated wt% to Mol% (Winter, 2010).

3. Results

3.1 Graphic logging:

The graphical logs of cores: AIA 370 (Figure 6a) and AIA 367(Figure 6b).

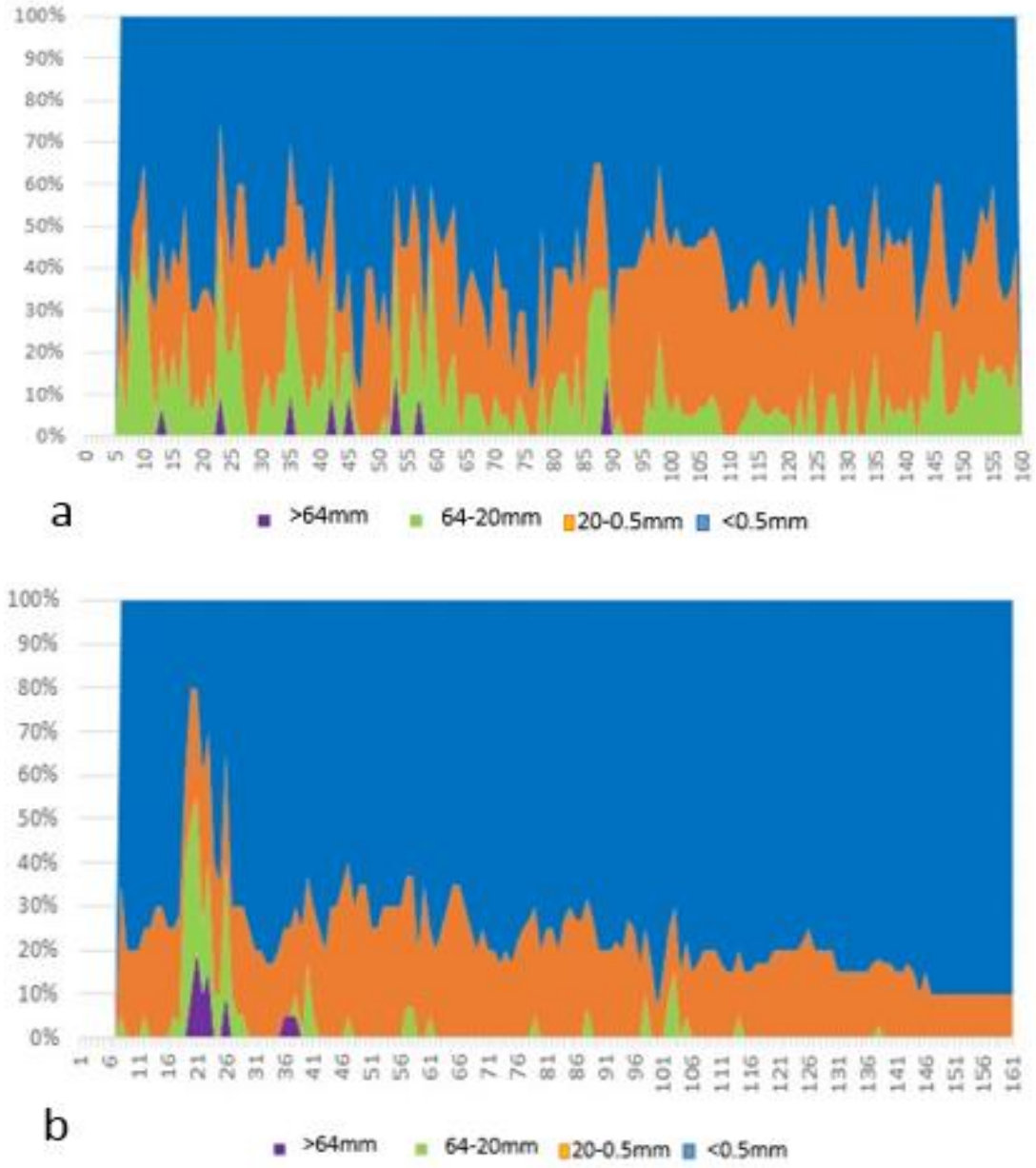

Figure 6. *Graphic logging of cores: a) AIA 370 (Hanging wall) and b) AIA 367 (Footwall). The Y-axis shows clast abundance in percent, X-axis show the core in m down core. Clast sizes over 2 mm show in purple respective green colour. Clasts under 2 mm detected by the eye show in orange colour, and matrix which was too fine grained to be observed by the eye are in blue colour.*

3.2 Petrography

3.2.1 Macroscopic

3.2.1.1 Hangingwall

The hanging wall is a porphyritic rock described as a grey- to darker grey coloured fine-grained matrix, containing scattered light coloured phenocrysts (0.5-2mm). Variable distributions of these pheoncrysts are seen in what seems to be grading structures. This is seen in larger and smaller scales from core to hand specimens (Figure 7).

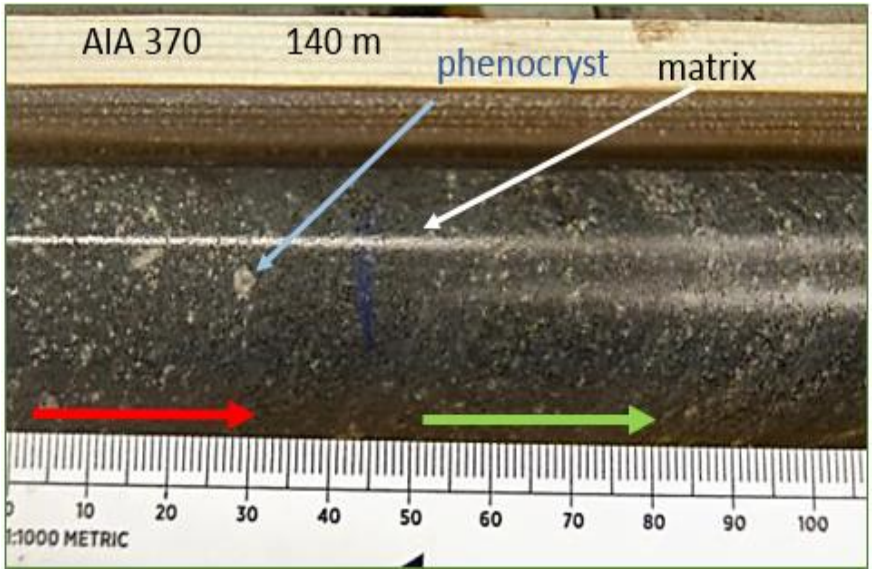

Figure 7. The porphyritic rock of the hanging wall. The red arrow shows decreasing in phenocrysts amounts, and the green arrow show increasing in phenocrysts amounts.

The porphyritic rock is supporting different poorly sorted clasts in sizes from 2-80 mm (shortening direction). Most of the clasts are distinct by the rounded flattened shape and by the colour of light or dark shades of grey (Figure 9). Clasts are also defined to be more subangular (Figure 9), and some are of a more compacted featured clast (Figure 8). Breccia clast are also found in the core. The clasts show commonly a preferred alignment. Distributed thin, elongated, dark minerals observed in preferred alignment indicate deformation of the rock.

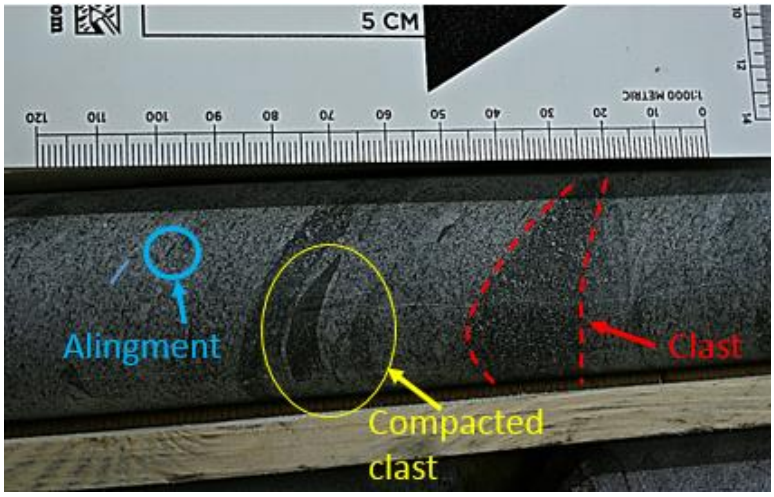

Figure 8. *The circle shows compact dark clast. Dashed marks show dark coloured subrounded clast. Hand specimens from AIA 370 at 35 m core depth.*

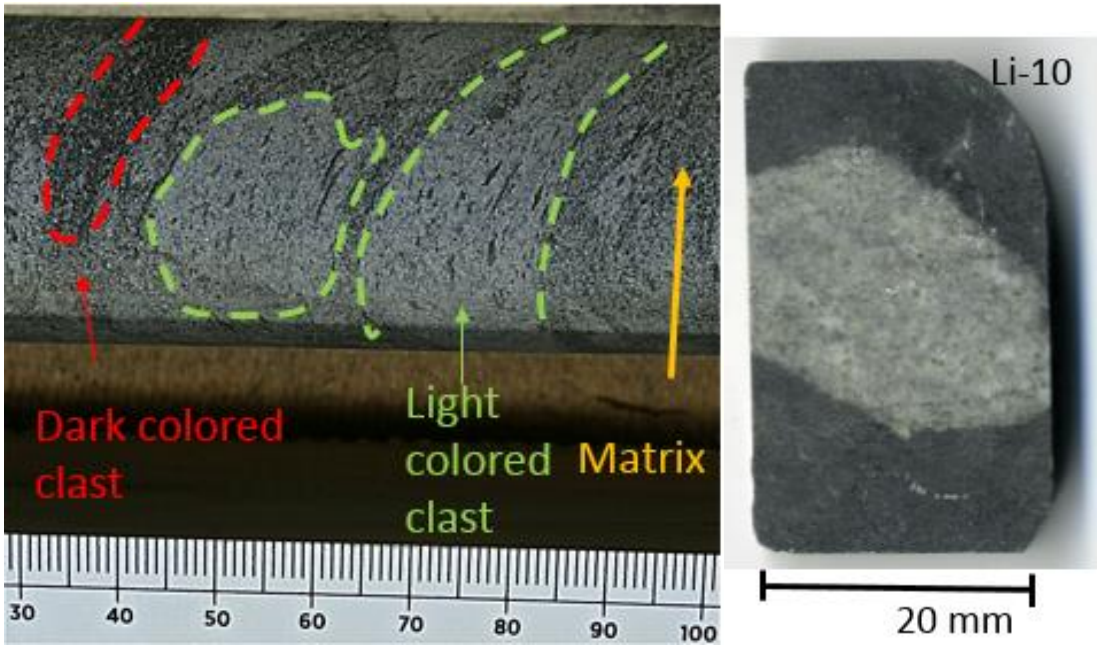

Figure 9. *Marker shows different clasts. Hand specimen: Li-10 shows a subangular fragment in cross section.*

3.2.1.2 Mineralization zone

The sample section from the mineralization zone comprise a fine-grained (0.5mm) grey –greenish coloured groundmass with scattered subrounded darker green coloured crystals of 0.5-3 mm. The crystals represent in general 35-40% of the rock (Figure 10). The scattered crystals show varied shades of green.

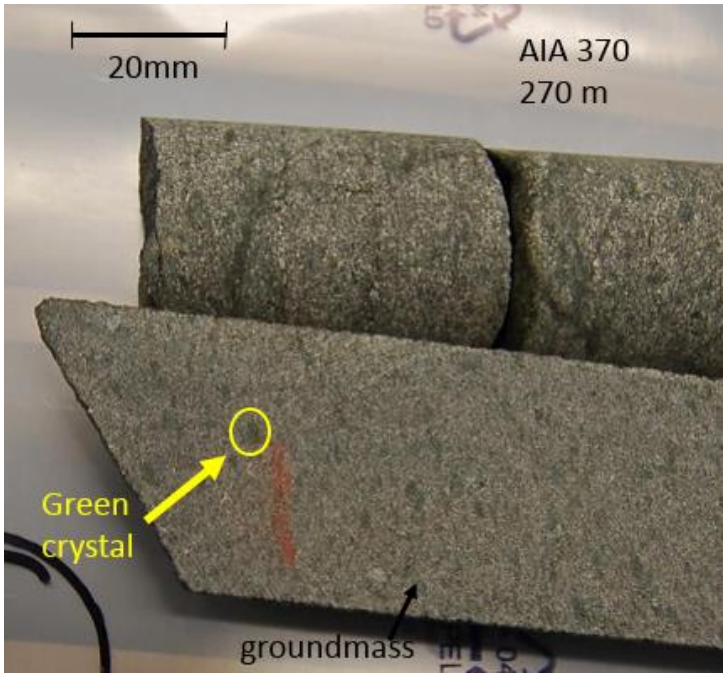

Figure 10. *Host rock in the mineralization zone shows green crystals in fine-grained groundmass.*

3.2.1.3 Footwall

The footwall shows a porphyritic texture of a dark grey coloured groundmass with scattered phenocrysts (0.5-2mm). The phenocrysts are distributed in the fine-grained matrix and show a slightly altered appearance. A section at 14 – 33 m core depth show well preserved, flattened, rounded, light grey coloured clasts (20-100mm, shortening direction) that are aligned parallel to the pervasive foliation (Figure 12). Few fragments were observed down core after 33 m and the core showed a more homogenous rock unit with depth (Figure 11).

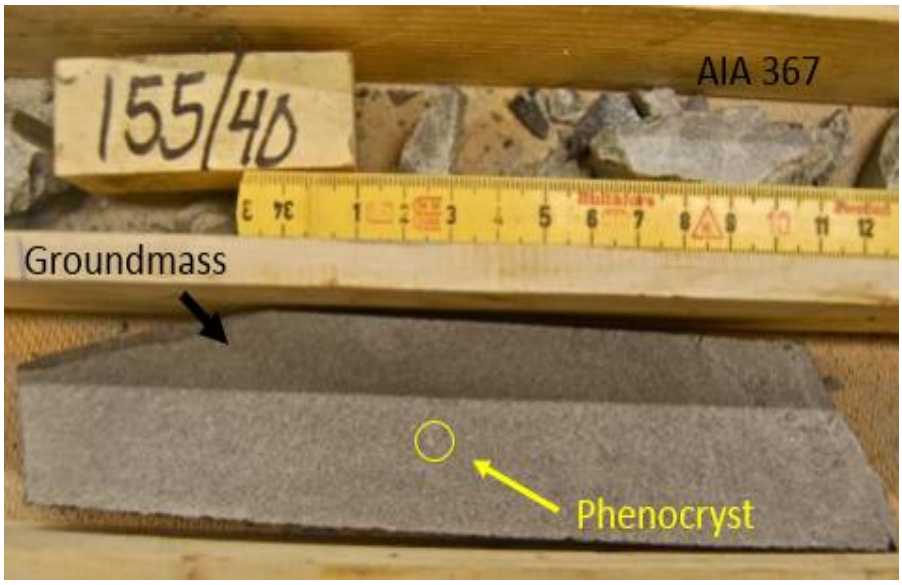

Figure 11. *Hand specimen from footwall (AIA 367) showing few phenocrysts at 156 meters core depth.*

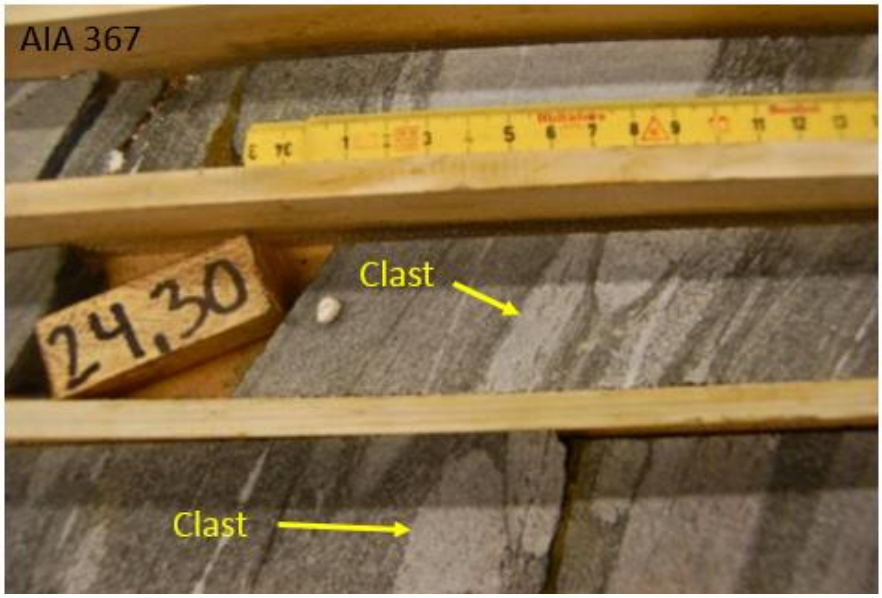

Figure 12. *Core AIA 367 showing flattened rounded clasts in a preferred alignment at 25 meter down core.*

3.2.2 Microscopic

3.2.2.1 Mineralogy

Microscopic observation of thin sections presented in table 1 as observed mineralogy. Table 2 represents mineralogy of different clasts. The thin sections are in order by the core depth.

ID core	Depth (m)	Sample no.	Quartz	Feldspar	Biotite	Amfibole	Epidote	Muscovite	Chlorite	Oxides	Calcite
AIA 370	13.40	Li-03	X	X	X	X	X		X	X	X
AIA 370	27.65	Li-04	X	X	X		X		X	X	
AIA370	59.70	Li-11	X	X	X	X	X		X	X	X
AIA 370	71.56	Li-13	X	X	X		X		X	X	
AIA 370	90.95	Li-14	X	X	X		X	X	X	X	X
AIA 370	96.20	Li-15	X	X	X		X		X	X	X
AIA 370	105.95	Li-16	X	X	X	X	X		X	X	
AIA 370	123.15	Li-17	X	X	X		X	X	X	X	
AIA 370	127.50	Li-18	X	X	X		X		X	X	
AIA 370	127.60	Li-22	X	X	X		X	X	X	X	
AIA 370	139.72	Li-19	X	X	X		X		X	X	
AIA 370	147.25	Li-20	X	X	X		X		X	X	
AIA 370	153.21	Li-21	X	X	X		X				
AIA 370	269.90	Li-25	R	XX	X	XX	X		X	X	X
AIA 370	274.90	Li-23	R	XX	X	XX	X		X	X	X
AIA 370	283.00	Li-24	R	XX	X	XX	X		X	X	X
AIA 367	89.30	Li-29	X	X	X	X	X		X	R	
AIA 367	155.75	Li-30	X	R	R	XX	X		XX	X	

Table 1. *Mineralogy of the groundmass. The "X" indicates that the mineral is present in the thin section, "XX" indicates that the mineral is increasing in the thin section. The "R" indicates that the mineral is reduced in abundance.*

ID core	Depth (m)	Sample no.	Comment	Quartz	Feldspar	Biotite	Epidote	Muscovite	Chlorite	Oxides	Calcite
AIA 370	10.61	Li-01	Light grey	X	X	R	X			X	X
AIA 370	12	Li-02	Light grey	X	X	X	R		R	X	X
AIA 370	27.65	Li-04	Compact			X			R	X	
AIA 370	28.6	Li-05	Compact			X			X	X	
AIA 370	31.35	Li-06	Light grey		X	X			X	X	
AIA 370	33	Li-07	Dark grey	X	X	X	X		X	X	X
AIA 370	35.58	Li-09	Dark grey	X	X	X	X			X	
AIA 370	36	Li-08	Green	X	X	R	XX		R	X	X
AIA 370	38.4	Li-10	Light grey	X	X	R	X	X	X	X	
AIA 370	61.3	Li-12	Green	X	X	X	XX		X	X	
AIA 370	102.9	Li-26	Breccia	R	X			X	X	X	
AIA 370	103.1	Li-27	Breccia	X	X			X		X	
AIA 367	18.5	Li-28	Light grey	X	X	X	X		X	X	X
AIA 367	60.9	Li-31	Light grey	X	X	R			R	X	

Table 2. *Mineralogy of distinct clasts. The "X" indicates that the mineral is present in the clast, "XX" indicates that the mineral is abundant in the clast. The "R" indicates that the mineral is reduced in abundances.*

3.2.2.2 Textures

Hanging wall

Thin sections from the hanging wall (Li-01 to Li-22) shows a microcrystalline matrix (<0.3mm) in with granoblastic texture of interlocking quartz grains. The matrix also includes grains of K-feldspar, biotite, epidote (Figure 13) and chlorite. Lath shaped biotite crystals define a weak foliation. The biotite is occasionally partely replaced by chlorite. Foliation of biotite shows alignment around feldspar phenocrysts with increasing depth along the core. Scattered phenocrysts of plagioclase occur in the groundmass. These crystals are mostly euhedral. The plagioclase are commonly poikilitic with epidote inclusions. The crystals commonly have polysynthetic twinning. Epidote was observed in all thin sections, but in minor amounts (< 5%). Epidote was also observed around oxides and biotite. Oxides include magnetite rimmed by hematite and occur disseminated throughout the samples.

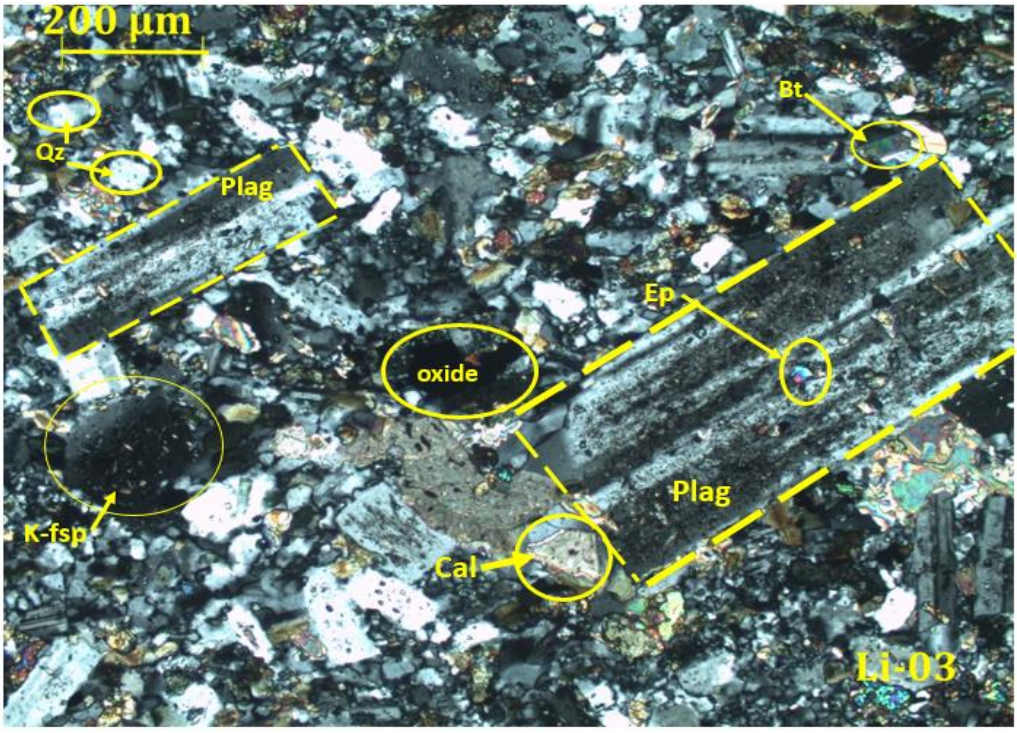

Figure 13. *A Micrography of sample Li-03 in cross polarized light. Table 3. Explains the mineralogy.*

Amb	Amphibole	K-fsp	K-feldspar
Bt	Biotite	Oxide	Magnetite
Chl	Chlorite	Plag	Plagioclase
Ep	Epidote	Qz	Quartz

Table 3. *Terms of mineralogy used in microphotographies.*

Amphibole is present in minor amounts, mostly in the upper hanging wall. The elongated subhedral amphibole grain is light green pleochroic, and shows a brownish colour in crossed polarized light (Figure 14 and Figure 24 in appendix). This is probably actinolite. Calcite is rare but appears disseminated in the matrix and in cross cutting veins. Muscovite was observed in a few samples replacing phenocrysts.

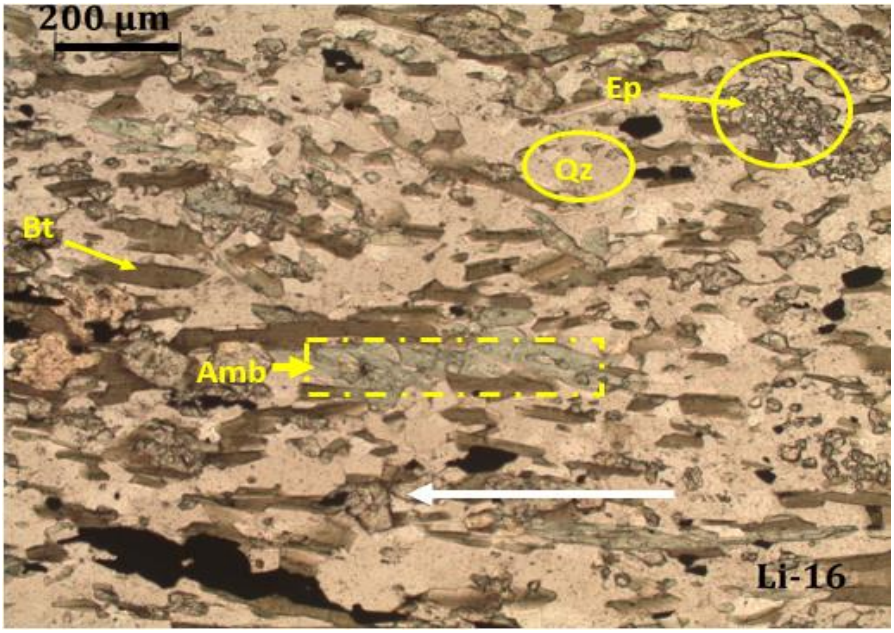

Figure 14. *A Micrography of sample Li-16 in plane-polarized light. Matrix of quartz, and biotite shows weak foliation (showed by arrow). Cluster of epidote and amphibole together with biotite.*

Mineralization zone

The matrix contains tight compressed microlaths (felty texture) (0.2-0.6 mm) in random orientation (Figure 15). The microlaths are euhedral interlocking plagioclase. Crystals of scattered amphiboles (>0.6 mm) were identified by the 60° cleavage angle, simple twinning and green pleochrism. The amphiboles are surrounded by biotite, chlorite, epidote, calcite and a minor amount of quartz grains (Figure 16). The amphiboles commonly have blue to darker green rims and a lighter green coloured core.

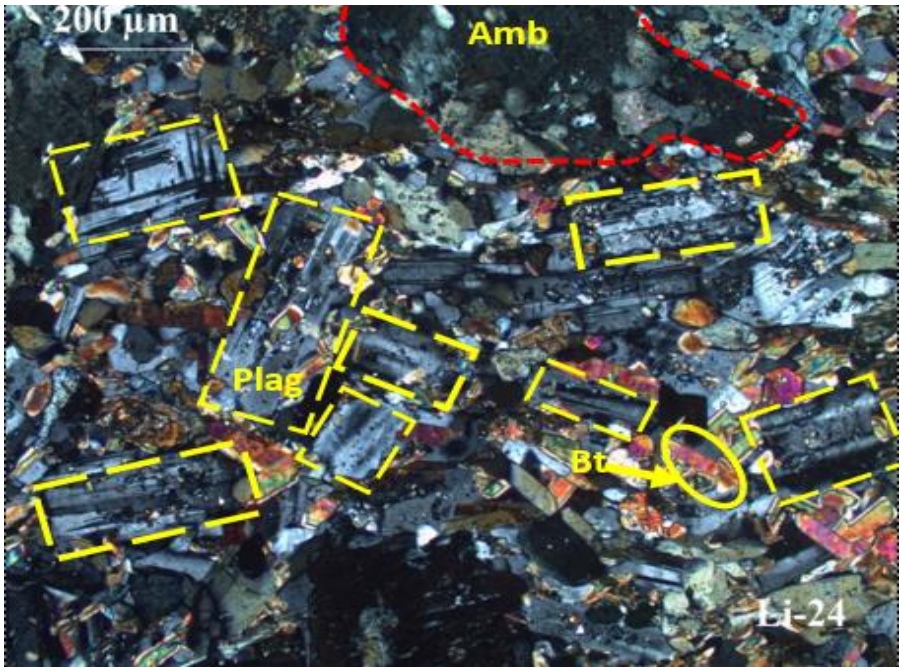

Figure 15. *A micrography of sample 24 in cross polarized light. Tight compressed microlaths in random orientation along with amphibole crystal.*

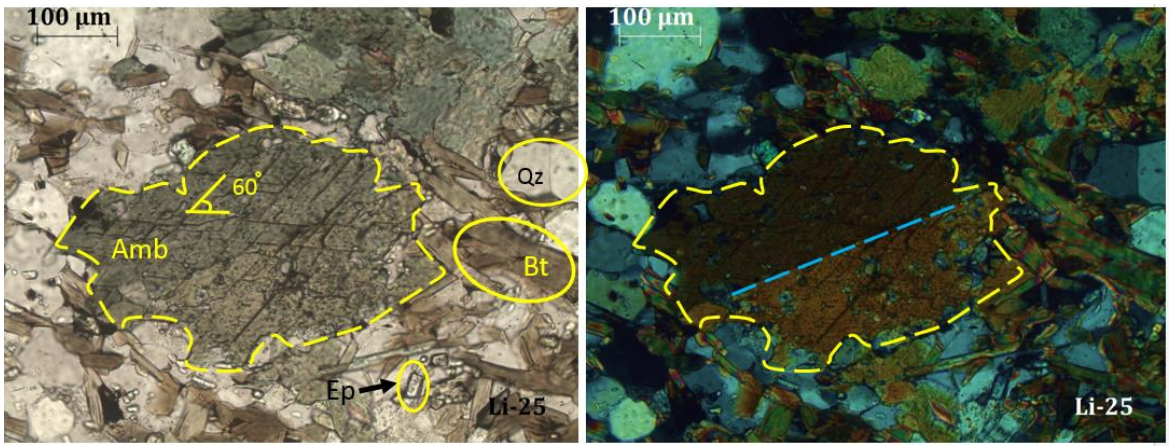

Figure 16. *A Micrography of sample Li-25 in plane- respective cross- polarized light. The amphibole shows clear cleavage and twinning (blue dashed line). The green amphibole is surrounded by brown biotite laths and epidote grains.*

Footwall

The matrix has a granoblastic texture of quartz grains and biotite. The lath shaped biotite shows weak foliation. Foliations intensity and the mode of amphibole increase down core (Figure 17). The biotite grains are less abundant and more altered with increasing depth along the core. Biotite is partly replaced by chlorite (Figure 17). The amphiboles are anhedral and show dark green pleochrism. Phenocrysts of plagioclase are altered with core depth. Relicts of possible quartz phenocrysts show a complete recrystallization to new quartz grains or K-feldspar grains (Figure 25 in appendix).

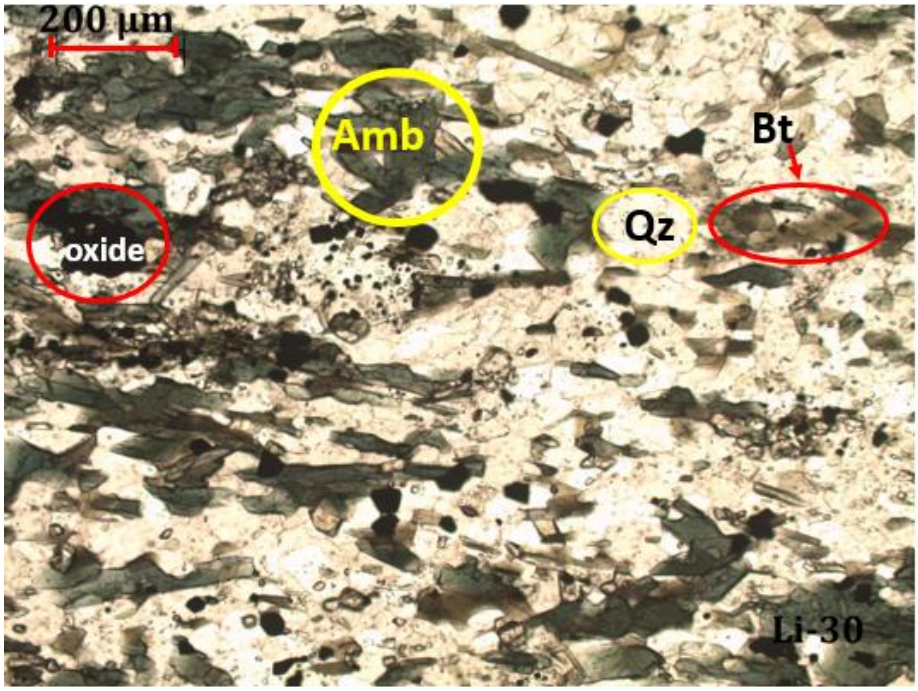

Figure 17*. A micrography in plane-polarized light of sample Li-30. The sample is amphibole rich, and biotite seems altered to chlorite. Mineralogy explained in table 3.*

Clasts

The clasts which are observed in the hanging wall and footwall commonly have a micrographic granoblastic texture of interlocking quartz grain and scattered phenocrysts. The phenocrysts are plagioclase. The plagioclase is euhedral and has a poikilitic texture. Some of the phenocrysts in the clast show zoning (Figure 18). Dark coloured clasts have a similar texture to the light coloured clasts. The difference is a higher content of biotite grains (Figure 19). Green pebbles contain a high amount of epidote. The dark compacted clast shows a compacted biotite rich assemblage with minor amount of oxides (Figure 26 in appendix). Breccia clasts (Li-26 and Li-27) show a brownish cryptocrystalline matrix in plane polarized light. This matrix supports angular clast with textures similar to the light coloured fragments.

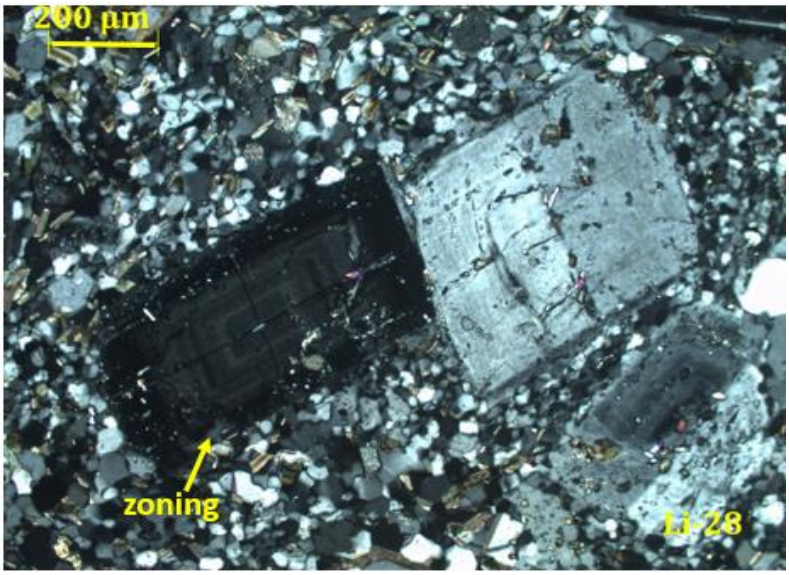

Figure 18. *A microphootgraphy in crossed polarized light of sample Li-28. The euhedral plagioclase show distinct zoning in a matrix of microcrystalline quartz and biotite.*

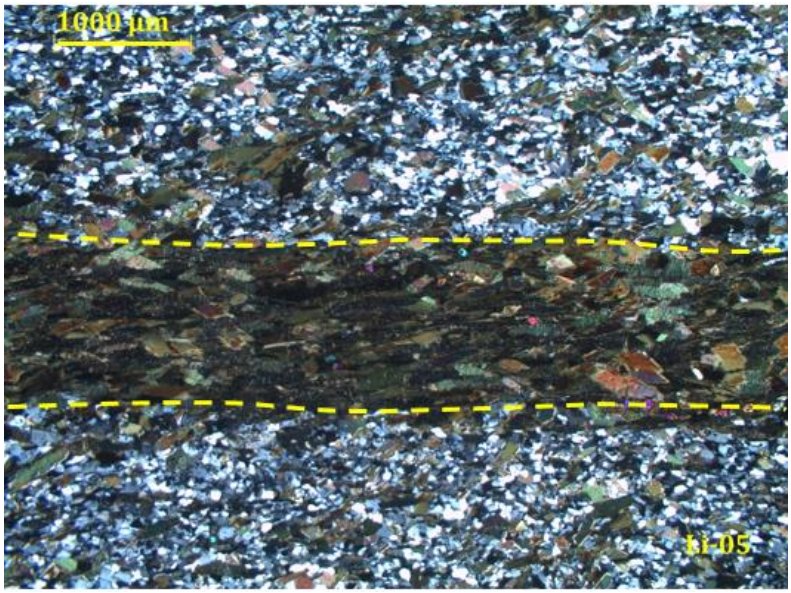

Figure 19. *Compacted fragment showed in microphotography of sample Li-05 in crossed polarized light.*

3.3 Geochemical analyses

Sample No.	SiO2	Al2O3	Fe2O3	MgO	CaO	Na2O	K2O	TiO2	P2O5	MnO	Total
1	62.13	16.84	6.02	2.7	3.47	4.94	3.11	0.52	0.18	0.11	100.02
2	62.64	16.68	5.53	2.27	3.99	6.16	1.87	0.54	0.19	0.12	99.99
3	60.68	17.13	6.03	3.06	3.69	6.13	2.4	0.56	0.2	0.14	100.02
4	55.76	19.26	7.43	4.79	4.35	3.72	3.77	0.55	0.21	0.17	100.01
5	63.04	16.86	5.72	2.42	4.01	4.97	2.19	0.5	0.19	0.11	100.01
6	63.25	16.9	6.11	2.13	3.42	5.57	1.86	0.5	0.18	0.08	100
7	59.14	17.62	8.05	3.35	3.6	5.03	2.27	0.6	0.22	0.11	99.99
8	59.48	17.24	7.15	3.34	4.79	5.1	1.9	0.66	0.23	0.11	100
9	61.7	17.1	5.96	2.44	6.09	4.45	1.44	0.53	0.19	0.09	99.99
10	61.79	17.71	6.17	1.68	4.39	4.08	3.34	0.51	0.21	0.1	99.98
11	59.68	18.48	6.33	2.79	4.46	4.95	2.51	0.51	0.19	0.1	100
12	59.86	17.29	6.76	2.98	6.36	4.51	1.28	0.61	0.22	0.12	99.99
13	58.78	18.11	7.41	3.54	4.18	4.22	2.86	0.59	0.2	0.13	100.02
17	59.37	17.35	6.52	2.7	7.33	3.96	1.87	0.58	0.19	0.13	100
14	60.74	17.41	7.08	2.91	3.93	4.76	2.28	0.59	0.2	0.1	100
15	60.94	17.36	7.18	2.91	4.49	3.98	2.26	0.57	0.18	0.12	99.99
16	59.43	17.34	7.43	2.51	4.87	5.23	2.24	0.64	0.2	0.11	100
18-20	52.23	14.99	10.74	7.14	9.02	2.45	1.99	1.01	0.21	0.17	100
21-23	58.13	16.42	9.16	3.63	5.54	3.58	2.32	0.87	0.18	0.12	100

Table 4. *The major and minor element in order down core, LOI-normalized to 100%. Geochemical samples with similar values are preserved as one average and these samples are: 18, 19, 20 (18-20) and 21, 22, 23 (21-23). Raw data and standards are shown in appendix. Sample: 1-17 Hanging wall (AIA 370), 18-20 – Mineralization zone (AIA 370) and 21-23 Footwall (AIA 367).*

wt%	Li-28 Grm	Li-28 Clast
SiO2	64.59	66.95
Al2O3	13.87	14.84
CaO	2.76	5.38
MgO	3.82	0.89
MnO	0.09	0.04
P2O5	0.09	0.10
Fe2O3	8.20	5.59
Na2O	2.67	3.87
K2O	3.24	1.68
TiO2	0.63	0.61
total	100.00	99.99

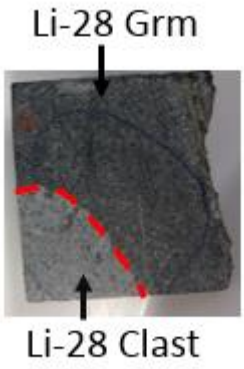

Table 5. *Geochemical analyses of major element. Sample Li-28 Grm, samples of the groundmass, and Li-28 Clast, is sample from the clast.*

3.4. Normative calculation

Sample No.	Quartz	Plagioclase	Orthoclase	Corundum	Diopside	Hypersthene	Rutile	Ilmenite	Hematite	Apatite	Sphene	Total
1	10.85	56.39	18.38		0.05	6.7		0.24	6.02	0.42	0.97	100.02
2	9.6	64.46	11.05		3.74	3.92		0.26	5.53	0.44	0.99	99.99
3	4.99	64.01	14.18		2.7	6.37		0.3	6.03	0.46	0.99	100.03
4	3.82	51.69	22.28	1.65		11.93	0.36	0.36	7.43	0.49		100.01
5	14.39	59.28	12.94		0.09	5.99		0.24	5.72	0.44	0.92	100.01
6	13.77	62.75	10.99			5.31	0.36	0.17	6.11	0.42	0.12	100
7	9.11	58.98	13.41	0.87		8.34	0.48	0.24	8.05	0.51		99.99
8	8.75	61.69	11.23		1.45	7.65		0.24	7.15	0.53	1.32	100.01
9	15.57	60.09	8.51		3.93	4.26		0.19	5.96	0.44	1.05	100
10	14.01	54.67	19.74			4.18	0.32	0.21	6.17	0.49	0.19	99.98
11	8.12	62.68	14.83			6.95	0.37	0.21	6.33	0.44	0.07	100
12	12.78	61.31	7.56		4.13	5.51		0.26	6.76	0.51	1.17	99.99
13	9.62	55.14	16.9	0.95		8.82	0.44	0.28	7.41	0.46		100.02
17	12.38	57.55	11.05		7.45	3.27		0.28	6.52	0.44	1.06	100
14	12.13	58.47	13.47	0.44		7.25	0.48	0.21	7.08	0.46		99.99
15	15.69	54.78	13.36	0.63		7.25	0.43	0.26	7.18	0.42		100
16	8.04	61.48	13.24		2.99	4.87		0.24	7.43	0.46	1.27	100.02
18-20	5.12	44.73	11.82		12.82	11.87		0.39	10.74	0.51	2.01	100.01
21-23	12.63	52.2	13.71		1.38	8.4		0.26	9.16	0.44	1.8	99.98

Table 6. *CPIW Normative calculation is present in wt%, obtained from the geochemical data in table 4.*

4 Discussion and interpretation of results

Zweifel (1976) suggested a sedimentary origin for the host rock of the Liikavaara Cu-Au deposit interpreted observations of clasts and inferred graded bedding. The hand specimens confirmed that rocks in the hanging wall and footwall contained clasts, which could support interpretation as a sedimentary conglomerate.

Zweifel (1976) implied that the geochemical data were not consistent with a sedimentary origin. A meta-sedimentary rock is likely to show variation in geochemical data cause by varied accumulation processes. The varied grading structures and beds seen in the graphic logging (Figure 6) would be comparable and corresponding to different sediment layers making up the protolith. The geochemical results (Table 4) showed a chemical variation in the hanging wall (sample 1-17), but in a narrow interval, example SiO_2 ranging between 56-63wt%.

However, the footwall showed a structure of a reversed grading by the graphic logging, which would indicate slight changes in sedimentation processes. The three geochemical data were quite consistent and were presented as an average for the whole core. If the rock would be of meta-sedimentary origin the sedimentation processes would be fairly homogenous in the footwall. Documented data of the graphic logging indicates clasts of <2-0.5 mm which seems to be the grading structures in the footwall (Figure 6b). The clasts of <2 mm were defined to scattered phenocrysts of plagioclase in the thin sections.

4.1 Interpretation of the host rock

To reach a conclusion, both petrological and geochemical results were interpreted together. The description of hand specimens showed a fine-grained, dark grey matrix with different observed clasts. The clasts were distinguished by colour and shape from the matrix. However, the mineralogy was too fine grained to observe by the unaided eye.

In thin sections the mineralogy of the hanging wall and the footwall shows a matrix that mainly consists of microcrystalline quartz grains and scattered euhedral lath shaped plagioclase phenocrysts. In the footwall the phenocrysts are more altered. This can indicate a higher deformation grade in the footwall, and also explain the reserved grading structure seen in the graphical logging. The plagioclase phenocrysts show alterations of epidote inclusions. The presences of epidote minerals can also be a good indicator of a volcanic protolith beacuse epidote is a common mineral in metabasaltic rock and less common in metapelitic (sedimentary rock) rocks (Bergman et al, 2001).

However, there were not many primary features in the rock preserved after the deformation events that have occurred in the area. The strongest evidence of an igneous protolith is the euhedral and zoned plagioclase phenocrysts. The euhedral shape indicates that the grain has not been transported by any sedimentary processes, but was

more likely a crystal growth in a slow cooling environment (Winter 2010) possibly in a magma chamber, which later could have erupted as a lava flow.

The samples from the mineralization zone are different from the hanging wall and the footwall. The fine-grained rock shows in thin section a felty texture (randomly oriented, tightly compressed microlaths) of euhedral plagioclase and crystals of amphibole. The rocks from the mineralization zone indicate a volcanic origin, more than a sedimentary origin. This interpretation is based on the low amounts of quartz grains observed in the thin sections compared to the rocks of the hanging wall and the footwall. The normative calculations (Table 6. sample 18-20) also indicated a low amounts of quartz (5.12 wt%). The definition of a sedimentary rock, is a rock formed during precipitation of minerals of processes as weathering, transport and deposition (Marshak 2008; Boggs, 2011). The euhedral plagioclase (Figure 15) does not seems to be weathered and transported.

Since the rock was metamorphosed which have caused change in the mineralogy, as well as too fine grained to observe in hand specimen, the mineralogy is calculated by normative calculation (Table 6). The result from normative calculation show an idealized mineralogy of low content of quartz (3-17 wt%), and high content of plagioclase (45-65 wt%).

The normative calculation is used in an aphanitic (fine grained igneous) rock diagram from IUGS for quartz (Q), plagioclase (P) and alkali feldspar (A). The samples plots in the andesite and basalt field (Figure 19).

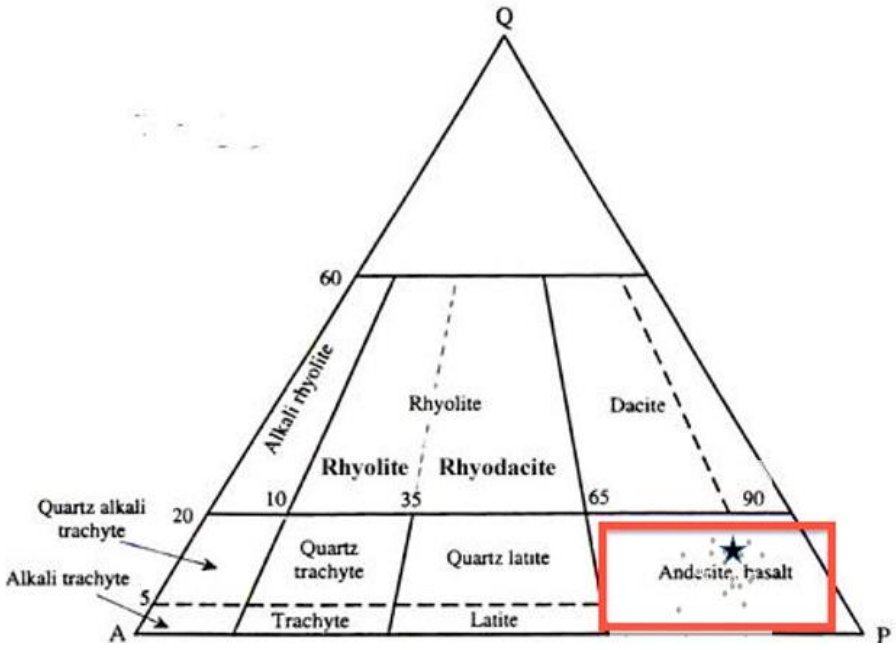

Figure 19. *Classification of an aphanitic igneous rock. Red box indicate the plotting area.*

If the rock is an andesite or basalt the rock would be volcanic. Generally in igneous rocks the geochemical result can be interpreted by the composition of SiO_2 wt%. Interpretation of the rocks point generally to intermediate composition (55-62 SiO_2

wt%),. By further identification of the rocks a classification in a TAS diagram from IUGS for volcanic rocks can be obtain from the geochemical data (table 4).

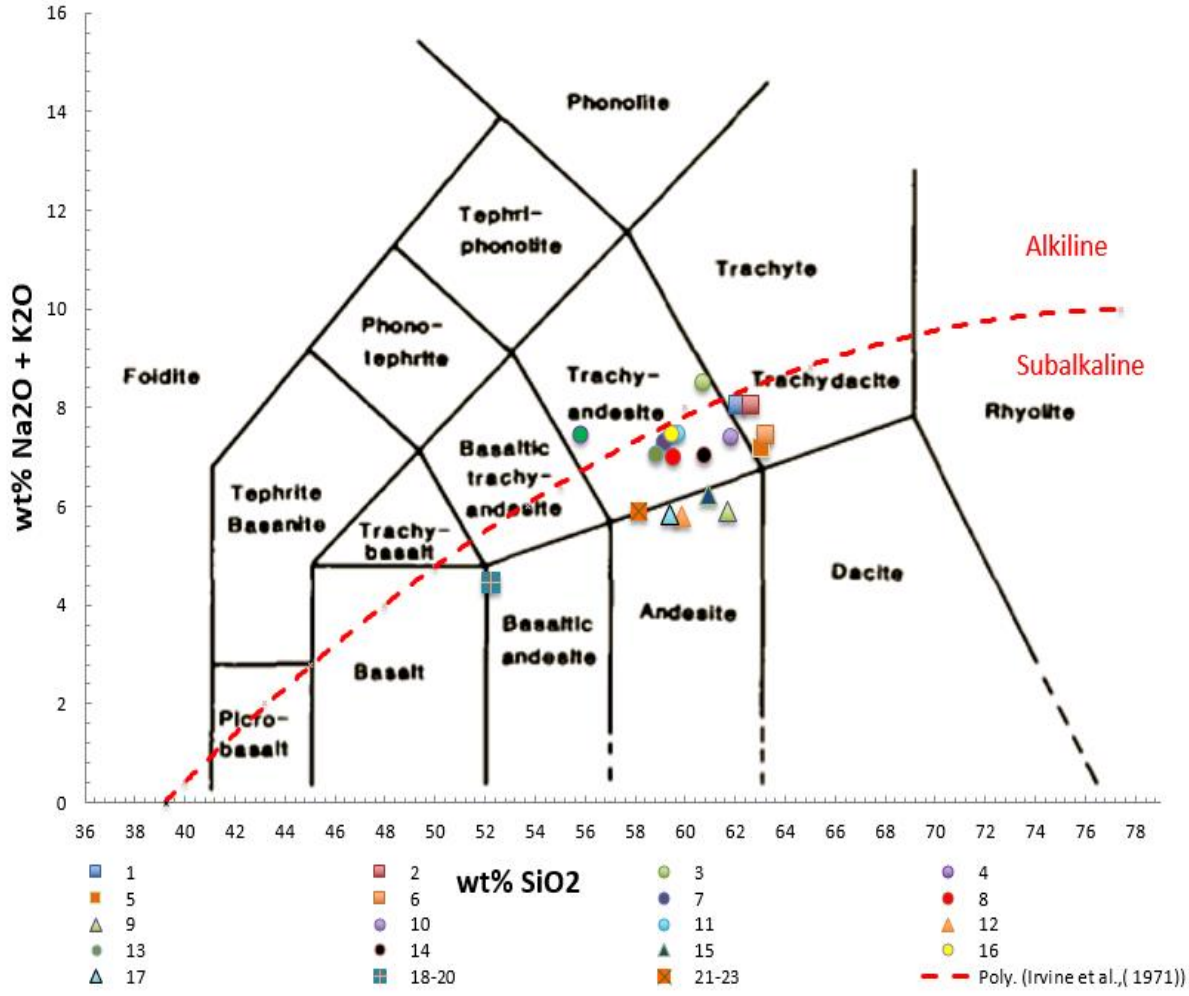

***Figure 20**. TAS diagram (Le Maitre, 1984) is used for further classification of the volcanic rocks based on 17 root names.*

The TAS diagram (Figure 20) shows that the data plot in the fields of trachy andesitic composition which confirms the IUGS classification in figure 19. The rock sample 18-20 represents the rocks from the mineralization zone, which shows a more basaltic composition than the other samples (Figure 21).

If the rocks are of volcanic origin, the clastic rocks are likely to be pyroclastic debris. A classification for pyroclastic rocks (Fisher R.V., 1966) can be applied from the data of the graphic logging (Figure 6). A pyroclastic rock refers to material composed of a volcanic source and deposited by eruption and aerial ejection from volcanoes (Fisher R.V., 1966).

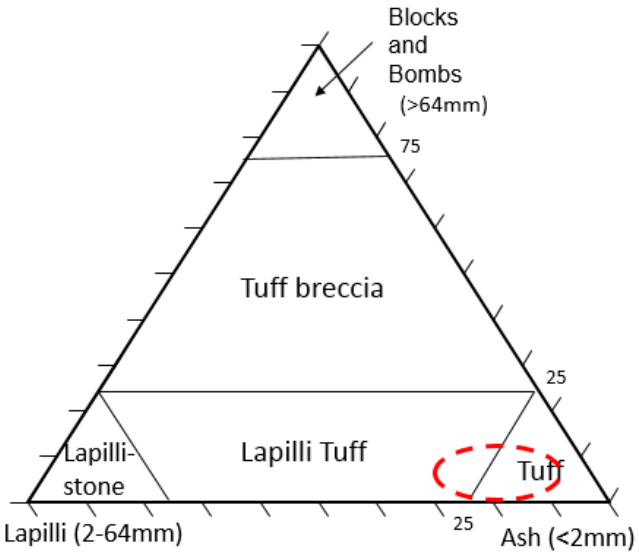

Figure 21. *The majority of the graphic logged meter sections (Figure 6) could be fitted in the lapilli tuff and tuff field.*

The graphic logged meter section in core AIA 367 (Figure 6b) contains an average content of >90% ash and core AIA 370 (Figure 6a) contains an average of 80-85% ash. The Interval of 6-90 m in core AIA 370 contains more lapilli and probably plots in the lapilli tuff field (Figure 20). The varied distribution of clast size can indicate pyroclastic eruption of different intensities.

Comparison of the clast and groundmass the geochemical analysis show a slight difference in SiO_2 wt% (Groundmass 64.6 wt%; Clast 67 wt%) and MgO wt% (Groundmass 3.8 wt%; Clast 0.9 wt%). In a volcanic rock the SiO_2 wt% and MgO wt% would indicate evolution of magma. An increasing of SiO_2 wt% and decreasing in MgO wt% content would suggest an evolved magma. If the clast is of volcanic origin and the groundmass is also volcanic origin, the geochemical data indicates that the clast is more evolved compared to the supporting groundmass. The clast contains zoned plagioclase phenocrysts (Figure 20). Zoning textures indicates change in temperature, normally that the temperature has dropped (Winter, 2010) during cooling in igneous rocks. Zoning (Figure 20) can also be caused by metamorphism (Winter, 2010). However an igneous origin is preferred for the following reasons: 1) the residual euhedral phenocrysts of plagioclase minerals. 2) Epidote, plagioclase and amphibole are common minerals in metabasalts. 3) A consistent andesite and basalt classification plot from geochemical data and normative calculation.

Probably the hanging wall and the footwall are related. These rocks may have been formed during the same process, most likely from an explosive volcano that has created lava flows that contained phenocrysts and ejected pyroclastic material. The aligned and flattened pyroclasts have most likely obtained the shape from the impact of ejection as it became deposited in a lava flow (McPhie, 1993).

4.2 Environment of formation

More information about the environment of formation can be obtained by magma series classification. Volcanic rock can be subdivided into alkaline and subalkaline magma series using a TAS diagram (Irvine and Baragar, 1971). Data from Liikavaara mainly plotted in the subalkaline field (Figure 20, in TAS diagram). The subalkaline magma series can be further subdivided using an AFM ternary diagram into tholeiitic and calc-alkaline series (Figure 22). The AFM diagram can be used to understand the evolution of the magma series. Samples that are plot closer to the MgO (M) corner (Figure 24) are expressed as less evolved magma (Irvine and Baragar, 1971).

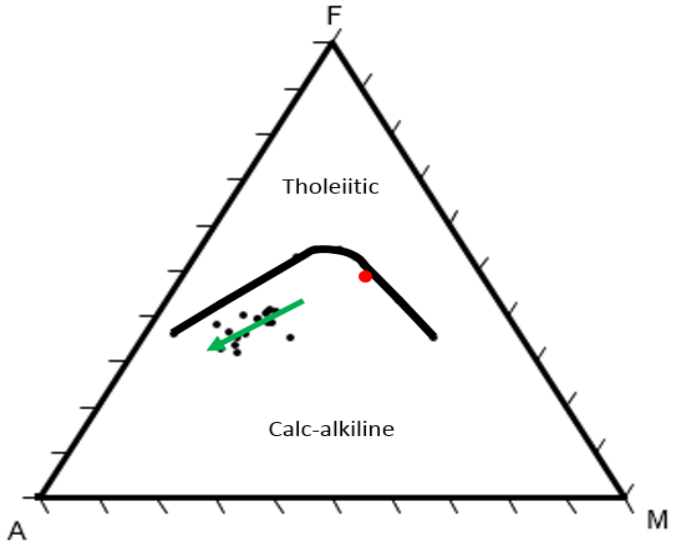

Figure 22. *AFM diagram. Red plot is distinct and show geochemical samples of 18-20 (Mineralization zone) (A=NaO+K2O, F= FeO and M= MgO; divide line Irvine and Baragar, 1971).*

The data from Liikavaara plotted in the field of calc-alkaline magma series (Figure 22). The geochemical samples of the mineralization zone (red plot in Figure 22) seem to be of a less evolved magma and differ distinct from the other samples (black plots in Figure 22). Convergent settings are related to calc-alkaline magma series. More specific the calc-alkaline series is typical of in subduction tectonic processes (Winter, 2010).

4.3 Metamorphic petrology

The rocks were metamorphosed. The mineralogy determine the temperature and pressure that rocks have been experienced. Metamorphism cause recrystallization of minerals in the rock. Quartz is a common mineral to form during metamorphism, and are able to be formed at low metamorphic grades (Philpotts and Ague, 2009). Microcrystalline quartz was observed in an interlocking grain texture and could be expressed further as a granoblastic texture caused by metamorphism (Winter, 2010).

Amphibole is preserved in all thin sections but most commonly in the footwall samples. The distinct elongated shape and the green pleochroic colour of the amphibole observed in the hanging wall suggests that this amphibole is actinolitic-hornblende.

A basaltic rock can be expressed by the geochemistry: SiO_2, Al2O3+Fe2O3 – (Na2O + K2O), C=CaO+3.3*P2O5 and F=FeO + MgO + MnO (wt%). This can further be plot in an ACF diagram for metabasaltic rocks. The presence of secondary epidote, chlorite and actinolite-hornblende indicate a mineralogy of greenschist facies (Philpotts and Ague, 2009). The plots in the ACF diagram (Figure 23) indicate that the bulk composition of the Liikavaara host rocks would be in equilibrium in the greenschist facies.

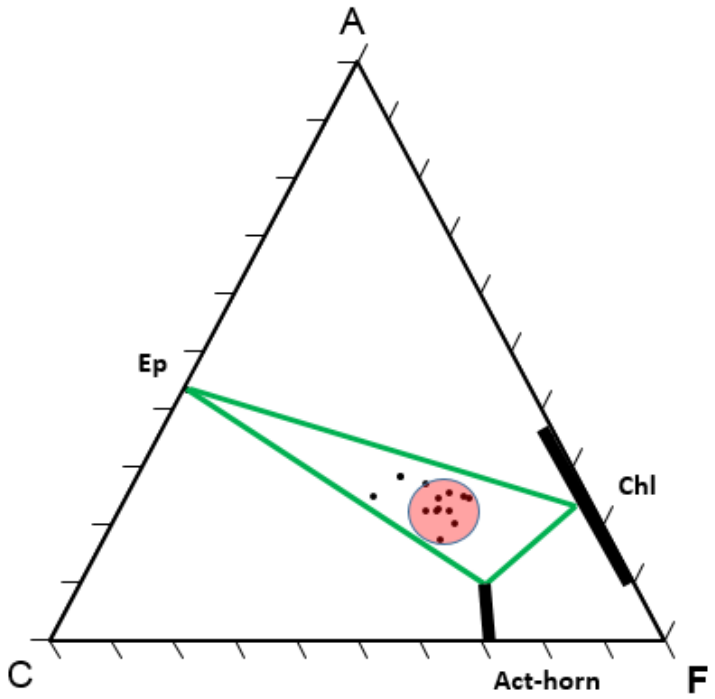

Figure 23. *ACF diagram showing that the geochemical composition of the rocks are fitting into upper greenschist field where epidote (Ep), chlorite (Chl) and actinolitic-hornblende (Act-horn) are plots (Philpotts and Ague, 2009).*

4.4 Evaluation of methods

Since samples were only collected from two cores of the Liikavaara deposit there is some question as to whether or not the results are applicable for the whole deposit. This could be determined by further analysis of additional samples from other cores within the deposit.

Sampling for primary rocks composition is difficult in rocks containing veins and alterations, which can affect the geochemical data analysis. For this reason it is good to compare several samples, and even from other cores. Errors in geochemical analyses can also depend on instrumental and standard errors.

Analysis of igneous rocks allows the chemical composition to be determined even if they are altered and metamorphosed. Chemical change due to metasomatism may make it difficult to determine the igneous protolith.

A microprobe analysis would have been useful, for example to get the composition of the plagioclase and figure out if the zoning is normal (cooling, Ca-rich core) or reversed (warming Na-rich core). by identify the element composing the core respective the rim (Winter, 2010).

5. Conclusion

The results from macroscopic, microscopic and geochemical data indicate that the host rock of Liikavaara Cu-Au deposit is of meta-volcanic origin. This interpretation is based on: 1) primary features of euhedral plagioclase 2) consistent geochemical data points towards an andesitic rock composition. From interpretation of thin sections and geochemical data, the rocks that comprise the mineralization zone seems to be a later rock formation possibly an intrusion of basaltic-andesite rock.

The geochemical data indicate an andesitic calc-alkaline magma which in turn indicates a subduction zone environment. This fits with the geological history of northern Norrbotten where subduction-related volcanism is referred to in other studies (Wanhainen et al., 2012; Bergman et al, 2001). A possible environment of the host rock would be a fore arc basin, which is commonly characterized by lava flows and pyroclastic material originating from a volcanic arc.

The metamorphic minerals indicate metamorphism in upper greenschist facies conditions. In conclusion the host rock of the Liikavaara deposit is an upper greenschist facies metaandesite and meta-andesitic tuff.

6. Acknowledgements

This project was financed by Boliden AB and I appreciate the opportunity to work with the project. A special thanks to Gregory Joslin who introduced me to the project, and Sofia Höglund for helping with the cores at Boliden AB, Gällivare. I would like to thanks for all guidance from Stockholm University, especially my supervisors Alasdair Skelton and Iain Pitcairn. I would also want to thank and Victoria Pease for good advices. Thanks to Dan Zetterberg and Runa Jacobson for help with practical work with my samples. A special thanks to Jonas Nilsson for good discussions and advices. Thanks to Ulrika Isvén for the support during this time.

7. References

Bergman, S., Kübler, L., Martinsson, O., 2001: *Description of regional geological and geophysical maps of northern Norrbotten County*. Geological Survey of Sweden. Ba 56, pp. 5–100

Boggs. S, 2011. *Principles of sedimentology and stratigraphy*. 5th ed. International ed. Pearson. new jersey, USA pp.2

Boliden annual report 2013, 2014: Boliden Mineral AB, Stockholm, 2014. pp. 38-42.

Eriksson J.A and Qvarfort U., 1996: Age determination of the Falun Copper Mine by 14C-datings and palynology. *GFF*, 118 (1), pp. 43-47.

Fisher R.V., 1966: Rocks composed of volcanic fragments and their classification. *Earth science reviews* 1. pp. 287-298.

Hollocher K., 2014: Normative calculation, excel spreadsheet. Geology Department, Union College, Schenectady, NewYork ,USA 12308.

Höglund S., 2014: Boliden cores. Boliden AB [conversation] (Personal communication, April 7th 2014).

Irvine T.N. and Baragar R.A., 1971: A Guide to the Chemical Classification of the Common Volcanic Rocks. *Journal of Earth Sciences*, vol. 8, pp. 523-548.

Johannsen, A., 1931: *Descriptive petrography of the igneous rocks*. Chicago: University of Chicago Press, p. 267

Le bas M.J. and Streckeisen A.L., 1991. The IUGS systematic of igneous rocks. *Journal of the Geological Society*, 148, pp.825-833.

Lehtinen, M., Nurmi, P..A. Rämö O.T,. 2005: Precambrian geology of Finland: key to the evolution of the Fennoscandian shield pp. 480-523

Le Maitre R. W., 1984. A proposal by the IUGS Subcommission on the Systematics of Igneous Rocks for a chemical classification of volcanic rocks based on the total alkali silica (TAS) diagram, *Australian Journal of Earth Sciences*, 31(2), pp. 243-255.

Marshak S. 2008. *Earth portrait of a planet.* 3rd ed. w.w.norton and company inc. New York, USA. pp .184.

McPhie J., 1993. Common components, textures and structures in volcanic deposits. ed. Doyle M., and Allen R.. *Volcanic textures: A guide to the interpretation of textures in volcanic rocks*. CODES key center, University of Tasmania. pp. 27.

Philpotts A.R. and Ague J.J., 2009. *Principles of igneous and metamorphic peterology*, second edition. Cambridge university press, Cambridge, pp. 447-472.

Wanhainen C., Broman C., Martinsson O., and Magnoe B., 2012: Modification of a Palaeoproterozoic porphyry-like system: Integration of structural, geochemical, petrographic, and fluid inclusion data from the Aitik Cu–Au–Ag deposit, northern Sweden. *Ore Geology Reviews* 48. pp. 306-331

Weihed, P., Arndt, N., Billstro K., Duchesne J.C., Eilu, P., Martinsson, O., Papunen, H., and Lahtinen, R., 2005. Precambrian geodynamics and ore formation:The Fennoscandian Shield. *Ore Geology Reviews* 27 (1-4). pp. 273–322.

Winter J.D., 2010: *Principles of igneous and metamorphic petrology*, second Ed., International Ed. Pearson, New Jearsy, USA, pp. 34 -687.

Yngström, S. Nord, A.G., and Åberg, G., 1986. A sulphur and strontium isotope study of the Aitik copper ore, northern Sweden. *Geology society. Stockholm Förh (GFF)*. 108 (4), pp. 367–372.

Zweifel, H., 1976: Aitik: geological documentation of a disseminated copper deposit – a primary investigation. *Geological Survey of Sweden*. C 720, pp.1-79.

Appendix:

ID Core	Thin section	Depth from	Depth to	ID Core	Sample No.	Depth from	Depth to
AIA 370	Li-01	10.61	10.74	AIA 370	1	10.43	10.61
AIA 370	Li-02	12	12.1	AIA 370	2	12.1	12.32
AIA 370	Li-03	13.4	13.5	AIA 370	3	13.5	13.68
AIA 370	Li-04	27.65	27.8	AIA 370	4	27.4	27.65
AIA 370	Li-05	28.6	28.67	AIA 370	5	31.2	31.35
AIA 370	Li-06	31.35	31.42	AIA 370	6	32.65	32.83
AIA 370	Li-07	33	33.1	AIA 370	7	35.67	35.83
AIA 370	Li-09	35.58	35.65	AIA 370	8	59.9	60.1
AIA 370	Li-08	36	36.07	AIA 370	9	71.35	71.56
AIA 370	Li-10	38.4	38.5	AIA 370	10	91.03	91.18
AIA 370	Li-11	59.7	59.77	AIA 370	11	96.27	96.45
AIA 370	Li-12	61.3	61.4	AIA 370	12	106.03	106.19
AIA 370	Li-13	71.56	71.63	AIA 370	13	128.5	128.66
AIA 370	Li-14	90.95	91.03	AIA 370	17	130.6	130.81
AIA 370	Li-15	96.2	96.27	AIA 370	14	139.5	139.72
AIA 370	Li-26	102.9	102.97	AIA 370	15	147	147.25
AIA 370	Li-27	103.1	103.25	AIA 370	16	153	153.21
AIA 370	Li-16	105.95	106.03	AIA 370	18	269.3	269.56
AIA 370	Li-17	123.15	123.25	AIA 370	20	277.05	277.3
AIA 370	Li-18	127.5	127.6	AIA 370	19	283.08	283.48
AIA 370	Li-22	127.6	127.74	AIA 367	21	21.84	22
AIA 370	Li-19	139.72	139.84	AIA 367	22	89.4	89.6
AIA 370	Li-20	147.25	147.34	AIA 367	23	155.85	156.1
AIA 370	Li-21	153.21	153.33				
AIA 370	Li-25	269.9	270.05				
AIA 370	Li-23	274.9	275.01				
AIA 370	Li-24	283	283.08				
AIA 367	Li-28	18.5	18.6				
AIA 367	Li-31	60.9	61				
AIA 367	Li-29	89.3	89.4				
AIA 367	Li-30	155.75	155.85				

Table 7. *Table over obtained samples in order by core depth: core, sample and depth. Li-number (01-31) show thin section and Samples 1-23 show geochemical analysis samples.*

STD SO-18	Standard	Standard	Expected	StdCalib0313	Standard	Expected
SiO2	58.13	58.16	58.47	SiO2	60.213	60.15
Al2O3	14.05	14.06	14.23	Al2O3	17.113	17.15
CaO	6.36	6.35	6.42	CaO	5.2326	5.27
MgO	3.40	3.41	3.35	MgO	1.7824	1.82
MnO	0.39	0.40	0.39	MnO	0.0996	0.1
P2O5	0.783	0.783	0.83	P2O5	0.551	0.49
Fe2O3	7.67	7.61	7.67	Fe2O3	6.8112	6.79
Na2O	3.69	3.68	3.71	Na2O	4.232	4.25
K2O	2.13	2.14	2.17	K2O	2.911	2.92
TiO2	0.694	0.688	0.69	TiO2	1.0542	1.07

Table 8. *Standard: STD SO-18, used by ACME laboratory. Standard StdCali0313, used by Stockholm University.*

Depth (m)	Sample no.	SiO2	Al2O3	Fe2O3	MgO	CaO	Na2O	K2O	TiO2	P2O5	MnO	LOI	Total
10.43	1	61.14	16.57	5.92	2.66	3.41	4.86	3.06	0.50	0.17	0.11	1.2	99.62
12.10	2	61.68	16.43	5.45	2.24	3.93	6.07	1.84	0.53	0.18	0.12	1.3	99.75
13.50	3	59.72	16.86	5.93	3.01	3.63	6.03	2.36	0.54	0.19	0.14	1.3	99.71
27.40	4	54.89	18.96	7.31	4.72	4.28	3.66	3.71	0.54	0.20	0.17	1.3	99.78
31.20	5	62.00	16.58	5.63	2.38	3.94	4.89	2.15	0.49	0.18	0.11	1.4	99.79
32.65	6	62.47	16.69	6.03	2.10	3.38	5.50	1.84	0.49	0.17	0.08	1.0	99.77
35.67	7	58.39	17.40	7.95	3.31	3.55	4.97	2.24	0.59	0.21	0.11	1.0	99.77
59.90	8	58.46	16.94	7.03	3.28	4.71	5.01	1.87	0.64	0.23	0.11	1.4	99.70
71.35	9	60.84	16.86	5.88	2.41	6.00	4.39	1.42	0.52	0.19	0.09	1.2	99.77
91.03	10	61.15	17.53	6.11	1.66	4.34	4.04	3.31	0.50	0.20	0.10	0.8	99.78
96.27	11	58.92	18.24	6.25	2.75	4.40	4.89	2.48	0.50	0.19	0.10	1.0	99.74
106.03	12	59.17	17.09	6.68	2.95	6.29	4.46	1.27	0.60	0.21	0.12	0.9	99.78
128.50	13	57.85	17.82	7.29	3.48	4.11	4.15	2.81	0.57	0.19	0.13	1.3	99.72
130.60	17	58.17	17.00	6.39	2.65	7.18	3.88	1.83	0.57	0.18	0.13	1.8	99.78
139.50	14	60.04	17.21	7.00	2.88	3.88	4.71	2.25	0.58	0.19	0.10	0.7	99.55
147	15	60.09	17.12	7.08	2.87	4.43	3.92	2.23	0.56	0.17	0.12	1.2	99.77
153	16	57.84	16.88	7.23	2.44	4.74	5.09	2.18	0.62	0.19	0.11	2.4	99.72
269.30	18	51.41	14.76	10.48	7.08	8.65	2.42	2.09	0.99	0.21	0.17	1.4	99.71
277.05	20	50.76	14.75	10.88	7.18	9.01	2.37	1.92	1.01	0.21	0.18	1.4	99.71
283.08	19	51.74	14.69	10.30	6.81	8.93	2.44	1.89	0.98	0.21	0.17	1.5	99.71
21.84	21	56.95	16.5	8.60	3.12	5.54	3.54	2.76	0.81	0.19	0.11	1.6	99.75
89.4	22	57.44	14.75	9.73	4.56	5.40	3.21	2.35	0.89	0.18	0.12	1.1	99.73
155.85	23	57.49	17.32	8.76	3.06	5.45	3.84	1.76	0.87	0.18	0.13	0.9	99.78

Table 9. *Raw data of geochemical samples in order with core depth. Samples 1-17obtained from hanging wall, 18-20 from mineralization zone and 21-23 from footwall.*

***Figure 24**. A micrography of amphibole from the hanging wall in crossed polarized light of thin section Li-03.*

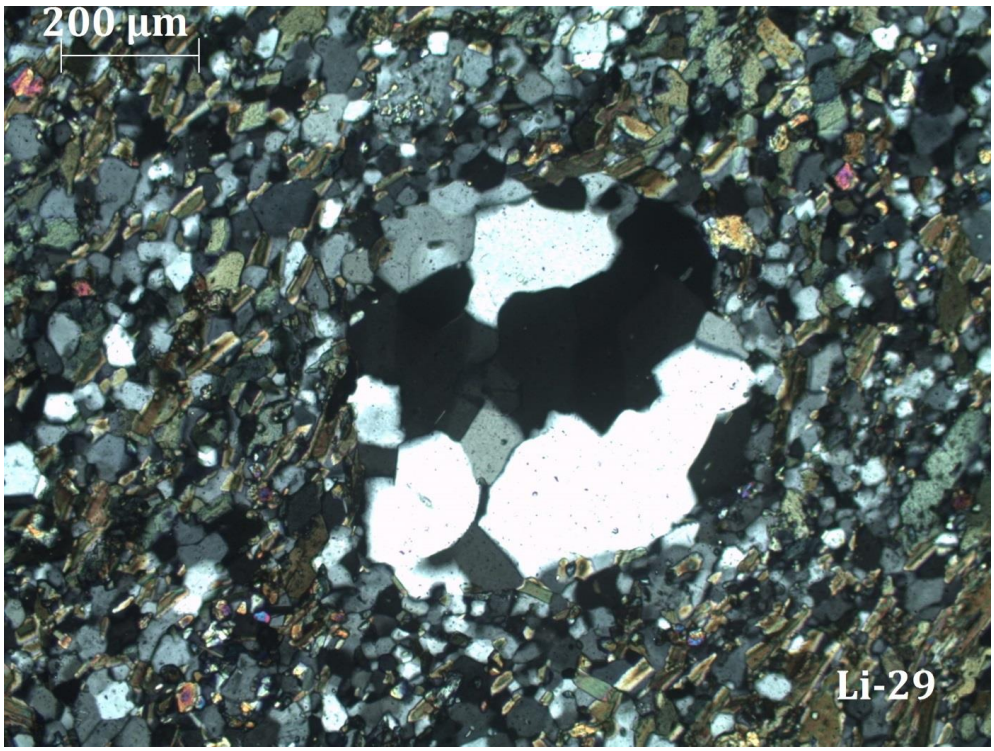

***Figure 25.** Microphotography of Li-29 in crossed polarized light. The relict phenocryst show recrystallized quartz grains.*